Sustainable water treatment: Harnessing mining waste as catalysts for Sicomet green degradation

Mohammed Kebir, Hichem Tahraoui, Imene Kahina Benramdane, Noureddine Nasrallah, Selma Toumi, Jie Zhang, Abdeltif Amrane

Water Resources and Industry 32 (2024) 100269

Contents lists available at ScienceDirect

Water Resources and Industry

journal homepage: www.elsevier.com/locate/wri

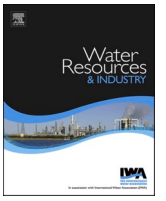

Sustainable water treatment: Harnessing mining waste as catalysts for Sicomet green degradation

Mohammed Kebir [a,b], Hichem Tahraoui [c,d,e], Imene Kahina Benramdane [f], Noureddine Nasrallah [f], Selma Toumi [c], Jie Zhang [g], Abdeltif Amrane [e,*]

[a] Research Scientific and Technical Center on Physico-Chemical Analysis (CRAPC), BP 384, 42000, Industrial Zone Bou-Ismail, Tipaza, Algeria
[b] Unite Research in Physical and Chemical Analysis on Fluid and Solid Medium (UR-APC-MFS/CRAPC), 11 Road Doudou Mokhtar, Ben Aknoun, Algiers, Algeria
[c] Laboratory of Biomaterials and Transport Phenomena (LBMPT), University of Medea, Nouveau Pôle Urbain, Medea University, 26000, Medea, Algeria
[d] Laboratoire de Génie des Procédés Chimiques, Department of Process Engineering, University of Ferhat Abbas, Sétif, Algeria
[e] National Center for Scientific Research (CNRS), National School of Chemistry of Rennes, University of Rennes, ISCR—UMR6226, F-35000, Rennes, France
[f] Reaction Engineering Laboratory, Faculty of Mechanical and Process Engineering, University of Science and Technology Houari Boumediene, BP32 El Alia, Bab Ezzouar, 16111, Algiers, Algeria
[g] School of Engineering, Merz Court, Newcastle University, Newcastle upon Tyne, NE1 7RU, UK

ARTICLE INFO

Keywords:
Mining waste
Photo fenton
Mineralization
Degradation
Sicomet green
Kinetic

ABSTRACT

This paper presents a novel circular economy approach to water remediation that focuses on creating sustainable systems by utilizing mining waste from El-Ouenza, Tebessa, in the east of Algeria. Waste materials are employed as catalysts in Fenton and photo-Fenton processes. Two cases were studied: the conventional and the modified heterogeneous photo-Fenton at a pH of 3 and under modified pH conditions for degrading Sicomet Green food dye ZS120. Catalysts were characterized through various analyses. Catalyst performance and dye degradation were examined for raw and calcined waste at 500 °C. Parameters like catalyst amount, sodium sulfite concentration, oxalic acid, and pH were optimized for both systems, with and without ligand. The first system achieved 91.5 % mineralization using 0.15 g L^{-1} catalyst, pH of 3, and 0.45 mM Na_2SO_3 in 90 min under sunlight. The second reached 78.5 % efficiency with variable conditions. Kinetic models demonstrated a first-order model for both photo-Fenton degradation and mineralization under sunlight. These findings guide eco-friendly dye degradation via mining waste-based catalysts in photo-Fenton systems, supporting sustainable wastewater treatment.

1. Introduction

The massive release of dyes into different water sources, such as rivers, lakes and oceans, is a major environmental problem that contributes significantly to the degradation of aquatic ecosystems [1–3]. Among the main players in this problem, the textile and paper

* Corresponding author.
E-mail addresses: medkebir@yahoo.fr (M. Kebir), hichemm.tahraouii@gamil.com (H. Tahraoui), kbenramdane@hotmail.fr (I.K. Benramdane), nas_nour@yahoo.fr (N. Nasrallah), toumiselma24@gmail.com (S. Toumi), jie.zhang@newcastle.ac.uk (J. Zhang), abdeltif.amrane@univ-rennes1.fr (A. Amrane).

https://doi.org/10.1016/j.wri.2024.100269
Received 31 August 2023; Received in revised form 22 September 2024; Accepted 26 September 2024
Available online 27 September 2024

industries, which largely depend on the intensive use of water for the fabric dyeing process, play a particularly worrying role in the aggravation of this pollution [4–6]. Indeed, the unregulated release of dye-contaminated wastewater into the environment can have devastating consequences, leading to contamination of water sources, disruption of aquatic ecosystems and compromised water quality for human consumption [7–9]. The historical use of colorants within various industries, including the food industry, the textile sector, cosmetics, paints, printing and inks, is of fundamental importance in creating an esthetically appealing product [10–13]. Indeed, colorants offer the possibility of infusing specific hues into finished products, thus helping to improve their visual and aesthetic characteristics [14–16]. These coloring substances are applied to many products, ranging from foodstuffs to clothing, cosmetics and plastic materials [17,18]. The aim of using these coloring substances is to enhance visual appeal, consolidate brand identity and positively influence consumer perception of products [19]. A concrete example in the field of food additives is Ponceau 4R, also referred to as Rouge Cochenille A and identified by the code E124 [20]. This red food coloring is artificially synthesized from raw materials of petrochemical origin. It falls under the food additive category E124 and belongs to the azo dye family, alongside other examples such as tartrazine (E102) and yellow-orange S (E110) [21]. These dyes share the common characteristic of having azo bonds associated with potential risks of teratogenicity [22]. It is essential to underline that using dyes across various industries requires rigorous regulation, particularly involving monitoring their concentration and nature [12]. This regulatory framework aims to guarantee consumer safety while minimizing potential environmental risks [23]. Many regions have thus introduced strict standards and regulations to govern the use of colorants in different products [24]. These guidelines are based on things like the Acceptable Daily Intake (ADI), whose recommendations are made by bodies such as in the Codex Committee on Food Additives and Contaminants (CCFAC) [25]. Efforts to minimize the effects of dye-induced pollution require an approach tailored to the specifics of dye types, their concentration in water, and environmental characteristics [26]. Thus, a range of depollution methods is implemented, encompassing the biological, physical, chemical and physico-chemical dimensions for the colored effluents treatment [27–32]. Biological approaches mobilize microorganisms such as bacteria and algae to break down dyes while subject to limitations inherent in specific conditions [33]. Physical methods, including filtration and settling, are aimed at separating dyes from wastewater. However, their effectiveness can be compromised in the presence of complex dyes and generate significant costs [34]. Chemical approaches involve using reagents to transform dyes into less harmful substances, but they can lead to the formation of unwanted by-products [35]. Physico-chemical methods combine different approaches to remove dyes, including coagulation-flocculation [5]. Among these solutions, heterogeneous photocatalysis stands out for its ability to decompose various organic pollutants, including persistent dyes, into less harmful products through the action of light-activated catalysts [36]. This method offers various advantages, such as complete removal of pollutants, mild processing conditions and the possibility of using natural light sources, thus enhancing its potential for sustainable waste management and environmental preservation [36]. In addition, numerous studies have explored mining-wasters' recovery using the Fenton method. One study developed effective catalysts for degrading ofloxacin in water using the $CuFeO_2$ (CFO) modified with polyvinylpyrrolidone (PVP) [37]. These catalysts showed superior performance in degrading ofloxacin, facilitated by increased oxygen vacancies and active sites. The findings improved understanding of catalytic mechanisms and reduced toxicity of intermediate products resulting from the ofloxacin degradation process [37]. In another investigation, researchers used magnetite fish scales and tea waste as adsorbents to capture Cu(II) ions and use them as heterogenous photo-Fenton catalysts for methyl orange degradation [38]. Furthermore, the catalysts showed high degradation efficiencies and stability, making them promising for wastewater treatment applications [38]. Another study found an effective recycling process for printed circuit boards containing copper using a two-step acid leaching method and eco-friendly synthesis of copper nanoparticles [39]. These nanoparticles were used as catalysts for surfactant degradation, achieving a 97 % copper recovery rate. These findings highlight the potential of recycled printed circuit boards for secondary copper sourcing [39]. A different study used pyrite from mine waste as a catalyst in a Fenton-like process to degrade tetracycline (TTC) [40]. The study identified essential oxidizing agents, degradation mechanisms, and operational parameters. The pyrite/H_2O_2 system facilitated TTC mineralization, with optimal conditions allowing 85 % mineralization within 60 min. Likewise, the procedure also improved human embryonic kidney cell viability, highlighting the practicality of using pyrite as a cost-efficient catalyst for TTC degradation and mineralization. It emphasizes insights from other relevant studies [40]. The reported study [41] evaluates advanced oxidation techniques, specifically photo-Fenton and ozone-based processes, for eliminating emerging contaminants of concern (CECs) in the Ibero-American region. The techniques include the complexation of iron with artificial and natural compounds, ultrasound-based hybrid methodologies, and ozonation techniques like peroxone, ultraviolet or solar light integration, and catalyst incorporation. In essence, the review assesses the efficiency of these techniques in eliminating contaminants from water matrices, considering strengths, limitations, and potential applications [41]. In a research endeavor, scientists used iron-rich industrial waste as catalysts in a photo-Fenton treatment process to treat water contaminated with Paraquat [42]. The study focused on various catalysts to break down Paraquat (PQ) in 25 mg L^{-1} samples. The findings affirm the viability of this waste-as-catalyst approach for remediating contaminated water [42]. Additionally, researchers developed a Fe_2O_3/BS heterojunction catalyst that degraded pollutants with 88 % PQ degradation and 82 % reduction in chemical oxygen demand (COD), leading to improved water quality [42]. An analysis of intermediates formed during the process was conducted using (liquid chromatography mass spectrometry (LCMS)to understand its mechanisms [42]. In a different investigation, the goal was to decipher the intricate degradation pattern of trimethoprim (TMP) and sulfamethoxazole (SMX) antibiotics in aqueous solutions under a photo-Fenton reaction, revealing that the reduction in SMX and TMP concentrations during the later phase is not solely due to competition between hydroxyl radicals and initial intermediates on antibiotic molecules [43]. Instead, the study highlights the importance of Fe(III)-antibiotic complexes in SMX and TMP degradation through photo-Fenton reaction, highlighting their impact on the efficiency and the potential of ferrioxalate complexes for process enhancement at neutral pH and low iron concentration level [43]. Another study explored using ferricarboxylates in a photo-Fenton reaction to treat antibiotic-contaminated water solutions containing Oxytetracycline (OTC) [44]. The process, which occurs under near-neutral pH conditions and solar irradiation, was found to be effective in preventing the formation of Fe:OTC complex and ensuring precise OTC

detection. The process also improved iron solubility, quantum yield, and light energy absorption. A pilot-scale CPC implementation successfully removed OTC, reducing *E. coli* activity and dissolved organic carbon [44].

Another study developed a novel mechanism using oxalate for controlling solid iron catalysts of Fe_3O_4@γ-Fe_2O_3 in heterogeneous UV-Fenton systems [45]. The composite was characterized using various methods, showing that oxalate induced significant iron leaching and promoted homogeneous UV-Fenton. The optimal oxalate concentration was found to be 0.5 mM, resulting in a pseudo-first-order rate constant of 0.314 min^{-1}, more than doubling the rate of the heterogeneous UV-Fenton system [45]. In a separate study, persulfate activated with ferrioxalate was utilized for lindane removal under simulated solar light and near-neutral pH conditions [46]. Results demonstrated complete lindane elimination in just 300 min using 0.12 mM of ferrioxalate and 2.29 mM of

Table 1
Comparison of the removal of organic compounds using various heterogeneous photo-Fenton systems.

Title	Contributions and limitations	References
Improved heterogeneous photo-Fenton-like degradation of ofloxacin through polyvinylpyrrolidone modified $CuFeO_2$ catalyst: Performance, DFT calculation and mechanism.	Composite of PVP/CFO catalyst was prepared through the modification of the $CuFeO_2$ (CFO) structure using polyvinylpyrrolidone (PVP), aiming to increase the oxygen vacancies by adding an active site to accelerate the formation of reactive radicals under light excitation. The prepared material exhibited significantly superior performance in degrading ofloxacin without limitation to the pH medium.	[37]
Catalytic activity of magnetite fish-scales and tea-waste as heterogeneous photo-Fenton catalysts for the removal of methyl orange through Cu (II) adsorption.	The study employed magnetite fish scales and tea waste as adsorbents to capture Cu(II) ions and subsequently utilize them as heterogeneous photo-Fenton catalysts for methyl orange degradation in aqueous solutions at an acid medium. The degradation efficiencies of 97.2 % and 96.9 % for Cu-MFS and Cu-MTW catalysts, respectively, were achieved.	[38]
characterization, and application of copper nanoparticles obtained from printed circuit boards to degrade mining surfactant by the Fenton process.	The preparation of copper nanoparticles from the recovery of printed circuit boards process, then their application as a catalyst for surfactant degradation by a Fenton-like process were reported. A 57 % degradation efficiency of total organic carbon of surfactant was achieved.	[39]
Use of mine waste for H_2O_2-assisted heterogeneous Fenton-like degradation of tetracycline by natural pyrite nanoparticles: Catalyst characterization, degradation mechanism, operational parameters and cytotoxicity assessment.	Degradation of tetracycline (TTC) with a heterogeneous Fenton-like pyrite/H_2O_2 process by pyrite from mine waste was reported. The study focused on crucial operating parameters such as pH and oxidant agents. It was found that more than 85 % of TTC was mineralized in 60 min and the maximum TTC removal was attained in the solution at an acidic pH value (4.1).	[40]
Developments in the intensification of photo-Fenton and ozonation-based processes for the removal of contaminants of emerging concern in Ibero-American countries.	The review delves into strategies applied in the photo-Fenton treatment technique, encompassing the complexation of iron with both artificial and natural compounds alongside hybrid methodologies incorporating ultrasound. Within the domain of ozonation, the study examines techniques that enhance the degradation of CECs, including peroxone, the integration of ultraviolet or solar light, and the incorporation of catalysts.	[41]
Abatement of paraquat contaminated water using solar-assisted heterogeneous photo Fenton like treatment with iron-containing industrial wastes as catalysts.	The work consists of treating PQ contaminated water using Fe-containing industrial waste as a catalyst via photo-Fenton treatment by utilizing iron-rich industrial waste as catalysts in a photo-Fenton treatment reaction achieved 88 % degradation of PQ and 82 % COD removal efficiency. The idea of using waste for treating waste serves the dual purpose of environmental remediation: treating wastewater and resolving the issue of solid waste disposal.	[42]
Enhancement of the photo-Fenton reaction at near neutral pH through the use of ferrioxalate complexes: a case study on trimethoprim and sulfamethoxazole antibiotics removal from aqueous solutions.	This study introduced ferrioxalate complexes for enhancing the photo-Fenton reaction of trimethoprim (TMP) and sulfamethoxazole (SMX) antibiotics, particularly at neutral pH (pH 5.0) and low iron levels (5.0 mg L^{-1}).	[43]
Process enhancement at near neutral pH of a homogeneous photo-Fenton reaction using ferricarboxylate complexes: Application to oxytetracycline degradation.	This work is mediated by ferricarboxylates for treating aqueous solutions containing the antibiotic Oxytetracycline (OTC) under solar irradiation. The reduced *E. coli* activity was achieved with an iron/oxalate molar ratio of 1:3, [Fe^{3+}] concentration of 2 mg L^{-1}, and an initial pH of 5.0.	[44]
Oxalate enhanced degradation of Orange II in heterogeneous UV-Fenton system catalyzed by Fe_3O_4@ γ-Fe_2O_3 composite.	This work involved the oxalate in the solid iron catalysts Fe_3O_4@γ-Fe_2O_3 in heterogeneous UV-Fenton systems. The degradation was 100 % after 20 min and after 120 min the total organic carbon was 86.6 %. The oxalate enhanced the heterogeneous UV-Fenton system of orange II.	[45]
Degradation of Lindane by persulfate/ferrioxalate/solar light process: Influential operating parameters, kinetic model and by-products.	The removal of lindane by persulfate activated with ferrioxalate under simulated solar lights and near-neutral pH conditions was reported. The results showed completely removing lindane in 300 min withing 2.29 mM persulfate and 0.12 mM ferrioxalate. Furthermore, chloride mineralization higher than 90 % is achieved under similar conditions.	[46]
Degradation of aqueous organic dye pollutants by heterogeneous photo-assisted Fenton-like process using natural mineral activator: Parameter optimization and degradation kinetics.	This work used natural minerals to remove methylene blue dye by photo-Fenton, showing that 91.3 % of degradation was achieved after 180 min.	[47]

persulfate, achieving over 90 % chloride mineralization [46]. The well-fitting kinetic model aids in predicting lindane removal in intricate scenarios [46].

In another study, researchers explored using natural catalysts to activate H_2O_2 in Fenton-based advanced oxidation processes to efficiently degrade organic pollutants [34]. A cost-effective, eco-friendly natural mineral was used to break down methylene blue (MB) dye in water and the obtained results revealed promising catalytic potential for large-scale dye wastewater treatment [47]. The effects of mineral composition, initial pH, catalyst quantity, and dye concentration were analyzed. Moreover, The pseudo-first-order kinetic model accurately predicted MB degradation with $R^2 > 0.98$ [47]. The study also discussed the potential mechanism of the heterogeneous photo-Fenton oxidation process [47].

In recent decades, numerous studies in the literature have explored various methods to enhance the efficiency of the heterogeneous photo-Fenton process for treating wastewater contaminated with emerging organic pollutants. These studies aim to overcome the limitations associated with using chemicals for iron sources or pH acidification. Table 1 provides a concise summary of the different investigations.

This paper presents a more sustainable and innovative approach for food dye remediation, mitigating their environmental impact. Within the scope of this research endeavor, the central focus was on harnessing the circular economy principles of development through the resourceful utilization of natural iron mining waste collected from El-Ouenza, Tebessa, in the northeastern region of Algeria. The primary motivation of this pursuit is to leverage the potential of this mining waste as a catalyst or efficacious support within the realms of the heterogeneous photo-Fenton and the modified heterogeneous photo-Fenton processes under sun light irradiation as a renewable energy source. This is a novel and unprecedented environmentally friendly approach to water remediation. The study comprised two distinctive aspects: firstly, the exploration of the conventional heterogeneous photo-Fenton process conducted under the regulatory constraints of a pH level set at 3, and secondly, the examination of a tailored heterogeneous photo-Fenton process characterized by an unconstrained pH by adding carboxylic such as the oxalic acid as a ligand of iron, aimed at the degradation of Sicomet Green (SG). The comprehensive characterization of the catalyst materials was diligently undertaken through an array of sophisticated analytical techniques encompassing X-ray diffraction (XRD), X-ray fluorescence spectroscopy (XRF), Fourier transform infrared spectroscopy (ATR-FTIR), scanning electron microscopy (SEM), UV–vis diffuse reflectance analyses, Brunauer-Emmett Teller (BET) method for surface area analysis, and thermogravimetric and differential analysis (TGA/DTG).

In addition, a meticulous assessment of the efficacy of these catalyst materials was executed, followed by practical investigations involving the photodegradation of dye treatments. This investigative phase also involved a comparative analysis of the deployment of raw and calcined mining waste, with the latter subjected to thermal treatment at a temperature of 500 °C. A series of systematic experiments aimed at optimizing critical parameters were carried out. These parameters encompassed the quantity of catalyst employed, sodium sulfite, oxalic acid concentration levels, scavengers and the modulation of the medium's pH. The ultimate goal of these optimization endeavors was to enhance the overall efficiency and performance of the processes under scrutiny.

Furthermore, the application of kinetic models was deemed essential to unravel the intricate nuances of the oxidation mechanism at play and elucidate oxidation mechanisms, further bolstering the scientific rigor of the research work. These nuanced and comprehensive findings reverberate with significant implications, presenting a promising avenue for integrating catalysts derived from mining waste within the heterogenous photo-Fenton system framework for degrading dyes in wastewater. Moreover, these research outcomes provide valuable guidance for the formulation of environmentally sustainable methodologies, via the photo-Fenton process under solar irradiation, for the degradation of dyes prevalent in wastewater. Central to its contribution, this work not only integrates circular economy principles, pioneers the utilization of mining waste, delves into dual study cases, conducts exhaustive catalyst characterization, meticulously optimizes parameters, and employs rigorous kinetic analysis, but also stands as an uncharted exploration, as no prior research has ventured into this realm. Collectively, these achievements pave the way for pioneering, sustainable, and exceptionally potent methods in dye degradation for wastewater treatment.

2. Materials and methods

2.1. Chemical reagents

The reagents used in this study are: Sodium bicarbonate $NaHCO_3$ (Sigma Aldrich, >99 %), Sodium chloride NaCl (Fluka, >99.5 %), Oxalic acid $C_2H_2O_4$ (Merk, ≥99 %), Isopropanol C_3H_8O (Merck, >98 %), Hydrogen peroxide H_2O_2 (Sigma-Aldric, 30 % w/v), 1.10 Phenolphthalein $C_{12}H_8O_2$ (Biochem, 99 %), Sodium acetate $C_2H_3NaO_2$. (Merck, 99.99 %), Iron sulfate $FeSO_4{\cdot}7H_2O$ (Merck, >99), Potassium fluoride KF (Fichersci, 98 %), Chloridric acid HCl (Sigma-Aldric, 37 %), Sulfuric acid H_2SO_4 (Merck, 98 %), Humic acid (Thermo Scientific, >98 %), Chloroform $CHCl_3$ (Merck), Sodium sulfite Na_2SO_3 (Sigma Aldrich, 98 %), Potassium nitrate KNO_3 (Merck, 99 %), Sodium sulfate Na_2SO_4 (Sigma Aldrich, >98 %), Potassium permanganate $KMnO_4$ (Sigma Aldrich, 99 %), and distilled water for preparing solutions. The dye was provided by an industrial food company, a stock solution of initial SG dye concentration was prepared and used during all the experimental runs. A known concentration of H_2O_2 solution was prepared with distilled water by diluting 30 % w/v of stock solution and stored in an amber-colored light-resistant glass bottle at a cold temperature. All chemical reagents in this work were used as received from the supplier companies.

2.2. Catalyst preparation and characterization

The raw iron mining waste was collected from the mine in El Ouenza region of Tebessa, northeastern of Algeria. It was dried at 100 °C to remove water, then crashed with a ball mill in a cylindrical agate container, and subsequently in an agate mortar to obtain a

fine powder. The fine powder was calcined in the oven at 500 °C under atmospheric air and the resulting iron mining waste powder was regrinding and homogenized. After that, it was subject to characterization such as Xray diffraction (XRD), Bruker D8 ADVANCE diffractometer, Scanning electronic microscope (SEM), Quanta TM 250 FEG SEM instrument, ATR-FTIR spectroscopy, Alpha One Bruker *Spectrometer*, chemical composition by X-ray fluorescence (XRF), Rijaku (ZSX Primus II USA) spectrometer, and diffuse reflectance solid (DRS) Analytik Jena's SPECORD Plus 200 spectrometer. The particle size of the sample is estimated by HORIBA Analyzer SZ-100V2. Surface area information was determined with Brunauer-Emmett Teller (BET) instrument (Micromeritics ASAP2020, USA). Thermogravimetric and differential analysis (TGA/DTG) was carried out on the TEA SDTQ 600 instrument up to 900 °C at a heating rate of 10 °C min^{-1} in atmospheric air. All the data of characterization are given in Fig. 1. The prepared sample was used in SG dye removal by heterogeneous photo-Fenton and the modified heterogeneous photo-Fenton processes.

2.3. Analytical methods

The analytical method of color removal was evaluated according to the decrease in absorbance using a double beam UV–Vis spectrophotometer (Shimadzu 1800, Japan) by taking the absorbance at maximum wavelength λ_{max} = 640 nm with the pH of the medium controlled by a HANNA pH meter (HI 2210). The removal efficiency of SG dye degradation is computed according to the following equation:

$$R(\%) = \left(\frac{C_o - C_t}{C_o}\right) * 100 \quad (1)$$

Where.

R: Degradation rate (%).
C_o: Initial concentration of dye (mg L^{-1}).
C_t: Concentration (mg L^{-1}) of dye at time t.

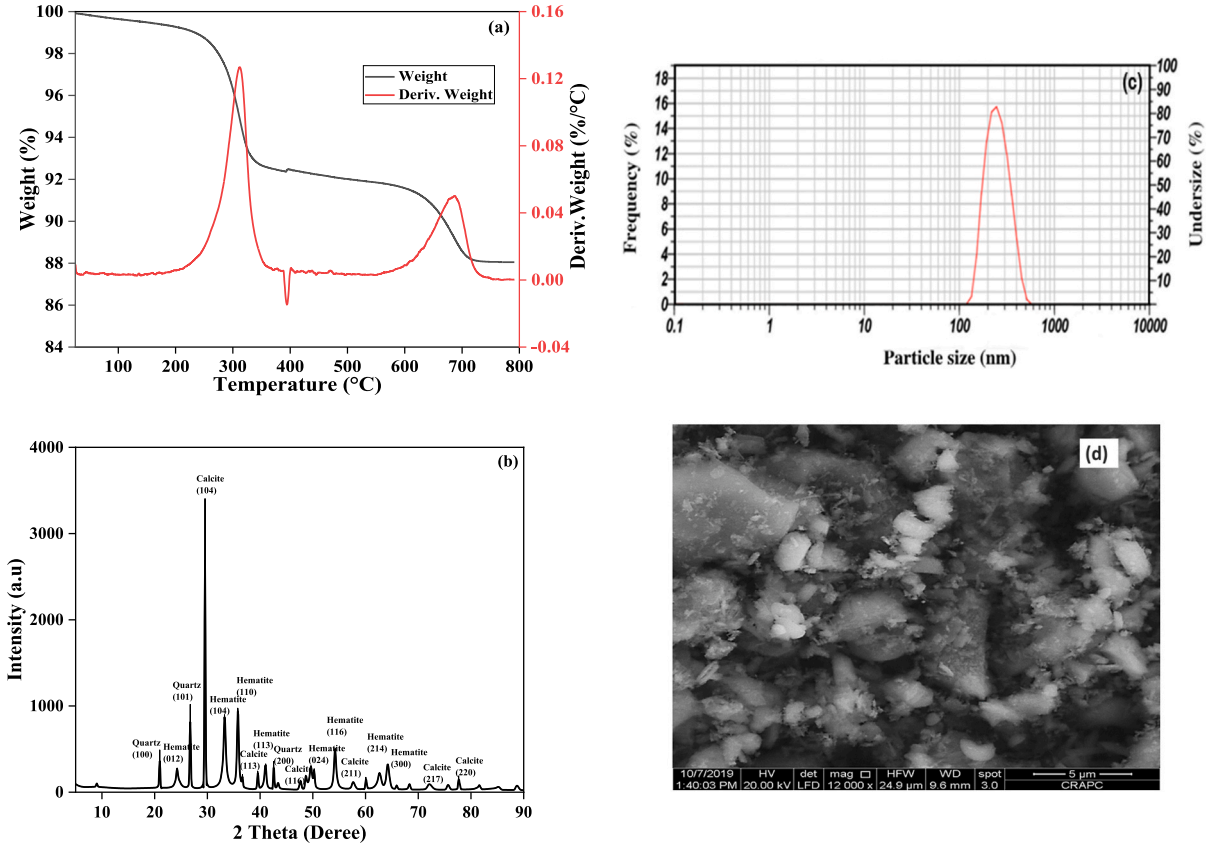

Fig. 1. Thermal behavior of raw iron waste, TGA-DTG profile (a), XRD patterns of calcined iron mining waste calcined at 500 °C (b), the particle size distribution of the calcined iron mining waste (c), SEM micrograph of iron mining waste calcined at 500 °C (d), ATR- FT-IR spectra of iron mining waste calcined at 500 °C (e), N_2 Adsorption–desorption isotherms iron mining waste calcined at 500 °C (f).

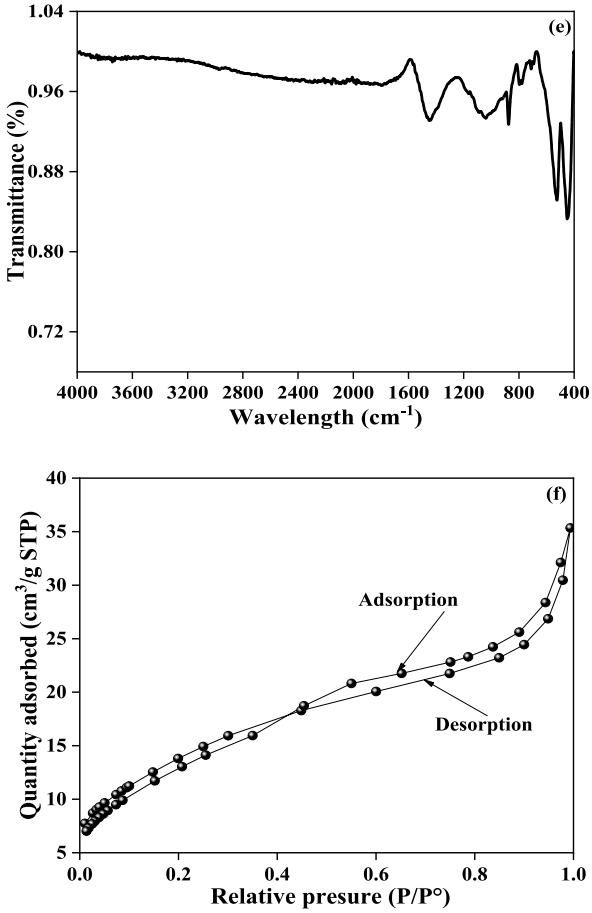

Fig. 1. (*continued*).

Chemical oxygen demand (COD) analysis for the collected samples was also assessed using Standard Procedures in water and wastewater.

Equation (2) was used to compute the mineralization rate.

$$\%\ COD = \left[\frac{COD_o - COD_t}{COD_o}\right].100 \tag{2}$$

where.

COD_o: initial chemical oxygen demand (mg O_2 L^{-1}).
COD_t: chemical oxygen demand at time t (mg O_2 L^{-1}).

3. Results and discussion

3.1. Structural and morphological characterization methods

Thermogravimetric analysis (TGA/DTG) was carried out using TEA Q6 equipment, with 15 mg of sample a temperature program up to 800 °C and a heating rate of 10°C/min.

The thermogravimetric analysis of the sample taken is depicted in Fig. 1(a), which illustrates the dehydration, decomposition and oxidation processes of powder of mining waste samples over time and temperature. The results of the thermal analysis of the raw mining waste indicate that, in the low-temperature range, the presence of an intense and large exothermic peak at 320 °C. This may also correspond to the deshydration and free water molecules evaporation on the surface of the powder. The release of the volatile matter corresponds to the desorption of water adsorbed in the pores inside the material. Another endothermic phenomenon of low intensity occurs at a temperature of 390 °C. It corresponds to the carbon dioxide loss derived from calcite and volatile material from the raw iron mining waste.

A small weight loss of 4 % is observed below 300 °C, possibly due to dehydration and free water molecule evaporation. It may also

correspond to the release of the volatile matter due to the desorption of water adsorbed in the pores inside the material and the decomposition of iron oxyhydroxide accompanied by an endothermic signal at around 380 °C [48,49]. The temperature range from 400 to 550 °C of thermal stability corresponds to the slight weight loss due to the formation of the hematite phase α-Fe_2O_3 [50]. A third exothermic peak appeared at around 680 °C of low intensity, corresponding to structural water of iron waste and associated minerals transformation [51].

X-ray diffraction (XRD) analysis can be used to study the crystalline structure of calcined iron ore. This analysis makes it possible to determine the crystalline phases of the iron ore catalyst and identify their composition. The XRD analysis was performed using Bruker D8 ADVANCE X-ray diffractometer, working with Cu Kα radiation ($\lambda = 1.54178$ Å). The data were collected over the range (2–90°) in steps of 5° (2θ) min^{-1} and presented in Fig. 1(b).

As shown in Fig. 1(b), the structure and the phase composition of the calcined iron mining waste demonstrates the presence of the most diffraction mainly related to the silica (ICDD 01-083-0539), hematite (ICDD0 01-076-9680) and calcite (ICDD 01-085-1108). The high percentage of hematite composition may be related to their photoactivity in the reaction of heterogeneous photo Fenton and modified heterogeneous photo Fenton.

X-ray fluorescence is based on the emission of characteristic X-rays by sample atoms when excited by high-energy X-rays. XRF elemental analysis of calcined mining waste enables the detection and quantification of chemical concentrations of numerous elements, from major to trace elements. Moreover, it provides valuable information which is essential for the study and characterization of materials. In this study, the XRF analysis was carried out by X-ray fluorescence spectrometry Rijaku (ZSX Primus II USA) and the analysis data are gathered in Table 2.

The iron oxide content of the calcined mining waste sample is quite high. According to the literature, iron is found in the form of oxides (Fe_2O_3) such as hematite and maghemite. The contents of SiO_2, CO_2, CaO and B_2O_3 are also very high. Magnesium, Barium, Zinc and Calcium can all be found in the structure of calcined ore.

The high Fe_2O_3, SiO_2 and $Ca(CO_3)_2$ content also suggests the presence of hematite, calcite and quartz in the calcined ore at 500 °C. Chemical analysis of the calcined mine waste sample also shows a relatively high sulfur content, suggesting the presence of gypsum.

A further investigation of the iron mining calcined by the analysis of diffraction scattering of laser light involves studying the scattering pattern produced when a laser beam interacts with an object or a diffracting medium by using HORIBA Analyzer SZ-100V2. This analysis provides information about the size properties of the powder of iron mining waste.

As observed in Fig. 1(c), the mean particle size of calcined iron mining waste powder was evaluated to be 246 nm. It is suggested that the iron mining waste powders after calcination can be considered as homogeneous composites.

The morphology of mining waste was conducted using a Quanta TM 250 FEG scanning electron microscope (SEM). The technique involves examining iron mining waste powder on a microscopic scale. It can also deliver information about the morphological structure of the calcined iron mining sample as can be seen from Fig. 1(d).

The SEM micrograph given in Fig. 1(d) shows a significant crystal of particles on the surface obtained after heating treatment of 500 °C for 2 h and becoming hematite, silica and calcite form. The dispersion of iron oxide can be appreciated in Fig. 1(d).

This analytical technique plays a significant role in characterizing and investigating material properties. In this work, ATR-FTIR analysis of the iron mining oxide obtained after calcination of the raw sample is a valuable technique, enabling the study of the structure and chemical composition of the sample to be analyzed. In addition, it consists of identifying the functional groups that occur during calcination.

Table 2
Chemical composition of calcined iron mining waste (oxide form).

Oxide	Result (% Weight)
B_2O_3	2.95
CO_2	10.99
Na_2O	0.04
MgO	0.78
Al_2O_3	2.18
SiO_2	13.78
P_2O_5	0.08
SO_3	0.15
K_2O	0.22
CaO	7.97
TiO_2	0.07
MnO	0.72
Fe_2O_3	59.32
NiO	0.01
CuO	0.02
ZnO	0.19
As_2O_3	0.15
SrO	0.02
MoO_3	0.01
BaO	0.25
PbO	0.08

As illustrated in Fig. 1(e), the ATR-FTIR spectra of the calcined iron mining waste exhibit several vibration bands that are mainly due to the presence of numerous elements. In addition, the main absorption-intensive bands of the prepared material appeared, hematite and calcite, which are characterized by Fe–O and O–C–O stretching vibrations, are situated at 524 cm-1 and 711 cm^{-1} respectively [52,53]. Moreover, the presence of Si–O stretching vibration is observed at 450 and 1039 cm^{-1}, the occurrence of silanol can be related to the quartz phase in iron mining waste [54], and the band at 874 cm^{-1} is attributed to the presence of Si– O – Fe, O–C–O or Mg–Al in the obtained powder iron mining waste [55,56]. Also, it can be reflected by the Si–O–Al group. Furthermore, the interlayer hydrogen bonding illustrates the possibility of hydroxyl linkage. Al–Mg–OH and Al–O–Fe bondings are reflected by the 779 and 820 cm^{-1} bands respectively. In addition, the peak at 779 cm^{-1} can be ascribed to the quartz [57,58]. The peak at 1450 cm^{-1} is attributed to the absorption carbonate group. Finally, the ATR-FTIR analysis confirms the existence of Fe bonding, which is necessary for the oxidation reaction of Fenton and photo Fenton.

The powder's specific surface area is determined according to the Brunauer–Emmett–Teller (BET) method using Micromeritics ASAP 2020 surface analyzer by physical N_2 adsorption and desorption at its liquefaction temperature (77 K) onto the solid's surface of mining waste powder by using 16.3 $Å^2$ for the cross-sectional area of N_2, which has been thoroughly degassed for 12 h to eliminate any remaining molecules of water and carbon dioxide prior the analysis. The experiment yields adsorption isotherms, whose morphology is contingent upon the adsorbate, the adsorbent, and the gas-surface interactions of the solid. The data of analysis are given in Fig. 1(f).

Fig. 1(f) illustrates the N_2 isotherm adsorption-desorption of the studied iron mining waste calcined at 500 °C, which exhibits isotherm type IV with H3-type asymmetric hysteresis loop, according to the classification of the International Union of Pure and Applied Chemistry (IUPAC). This pattern is characteristic of mesoporous materials that are composed of aggregate particles. The BET surface area of the iron mining particles was 50.63 m^2/g, while the average pore size was 49.436 Å of iron mining waste particles. The total pore volume for pores with a diameter smaller than 3096.038 Å at P/Po = 0.9937 was 0.054678 cm^3/g. These data confirm that the material exhibits a mesoporous structure as anticipated and is in good agreement with those reported in the literature [59].

To further determine the optical properties of the obtained iron mining waste, Solid UV diffuse reflectance analysis, a technique commonly used to determine the optical properties of solid materials in the UV and visible wavelengths range, was used. Generally, iron mining waste shows a high absorption of ultraviolet blue light as shown in Fig. 2(a) and the spectra of diffuse reflectance of iron mining waste is in good agreement with the spectrum obtained by Yamanoi et al. [60]. The diffuse reflectance spectra shown in Fig. 2 (a) indicate that the sample exhibited a band at about 750 nm due to the $^6A_1 \rightarrow {}^4A_2$ single electron iron transition in the hematite phase, which is more prominent in this sample because of the increase in the hematite content after the thermal treatment. For the other

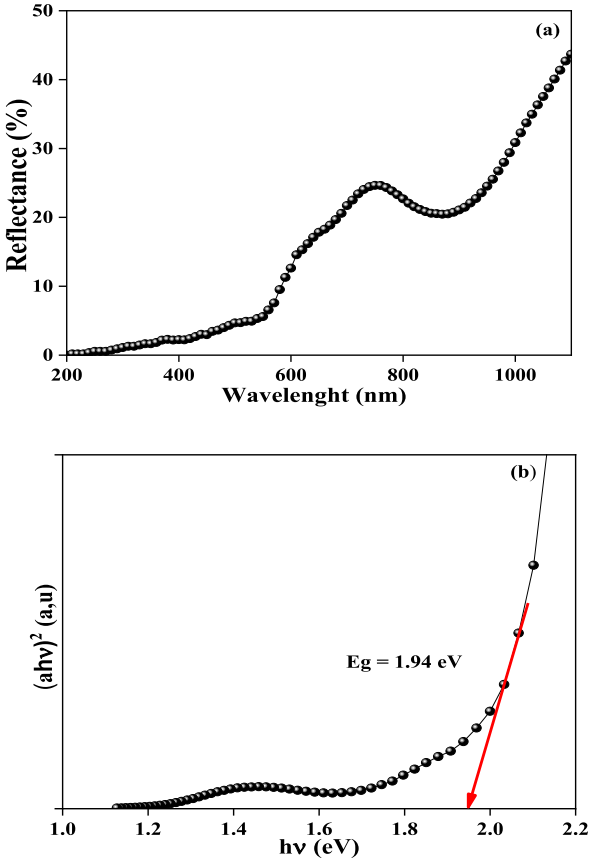

Fig. 2. Diffuse reflectance spectra (a) and Tauc plot of $(\alpha h\nu)^2$ versus photon energy ($h\nu$) for iron mining calcined at 500 °C (b).

remaining phases (SiO_2 quartz, $CaCO_3$ calcite), no band corresponds to them.

The diffuse reflectance spectrum of iron mining is presented in Fig. 2(b). The absorption intensities can be determined using the Kubelka–Munk equation [61] and the bandgap (Eg) is calculated from Tauc's equation [62]:

$$(\alpha h\nu) = Const^{*}(h\nu - Eg)^{n} \quad (3)$$

where α is the optical absorption coefficient, Eg is given from the plot $(\alpha h\nu)^n$ versus the incident energy ($h\nu$). The direct gap Eg of iron mining for $n = 2$ is evaluated at 1.94 eV by extrapolation of the linear parts of $(\alpha h\nu)^2$ versus $h\nu$ curves as shown in Fig. 2(b). The obtained value corresponds to the range of α-Fe_2O_3 reported in the literature and demonstrated an agreement with other reported studies [63]. The slight difference can be related to the quantum size effect.

3.2. Heterogeneous system study

At present, the heterogeneous photo Fenton system is a promising technology with interesting applications worldwide. It involves the investigation of solid active catalysts based on the direct or indirect absorption of light radiations in the reaction of photo-degradation of pollutants. Moreover, it offers a great advantage compared to other techniques in use to allow the total mineralization of pollutants, while respecting the integrity of the ecosystem.

The primary disadvantage of the classical photo Fenton (H_2O_2/Fe^{2+}) or photo Fenton modification (Iron/Lig) process is the fact that the soluble iron, added as a catalyst, cannot be retained at the end of the reaction, so it generates additional water pollution. To avoid the precipitation of dissolved iron, heterogeneous systems have been set up by using recyclable iron-based catalysts, such as iron mining waste.

In this section, we briefly present two processes. One is the classical heterogeneous photo-Fenton with a pH of 3 and the other is the application of the modified heterogeneous photo -Fenton process with an unadjusted pH in order to degrade the SG dye with a concentration of 10 mg L^{-1}.

3.2.1. Effect of the oxidants

In a Fenton or photo Fenton reaction, the choice of oxidant is important and depends on various factors such as the target pollutants, the operating conditions, and also the desired process efficiency. As it generates hydroxyl radicals (OH^-), which are the most reactive and play a crucial role in the oxidation of organic contaminants in various water treatment processes for environmental sanitation. Before starting the parametric study, the three most commonly used oxidants were tested including H_2O_2 hydrogen peroxide, Na_2SO_3 sulfite of sodium, and $K_2S_2O_8$ persulfate of potassium. The concentrations used were 0.15 mM at a pH medium of 3 and a solid catalyst amount of 0.1 g L^{-1}.

The degradation efficiency of the SG dye, as a function of different oxidants depicted in Fig. 3, shows that the photocatalytic activities of the iron oxide catalyst in the presence of 0.15 mM sulfate are lower than those of H_2O_2 and persulphate. A yield of 25 % was noted with sulfite, 17 % for H_2O_2 and 5 % for persulphate. According to these findings, sulfite promotes the degradation and mineralization of SG.

The low SG photodegradation yield in the presence of mining waste iron oxide under sunlight and with the addition of $K_2S_2O_8$ can be related to the role of SO_4^{-2} by scavenging the valuable hydroxyl radicals to form SO_4^{*-} [64]. Meanwhile, the hydroxyl radical (*OH) generated by the interaction between mining waste iron oxide and H_2O_2 plays a significant part in the photodegradation reaction of SG [65]. However, the improved photodegradation efficiency with Na_2SO_3 is due to the mining waste iron oxide which could play a critical role in enhancing Na_2SO_3 oxidation efficiency [66].

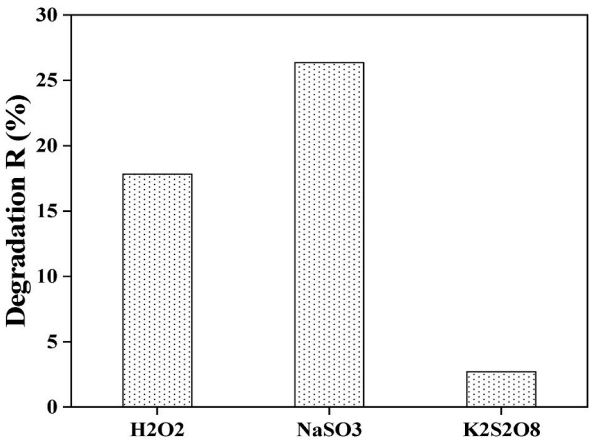

Fig. 3. SG dye degradation evolution for different oxidants by heterogeneous photo Fenton.

3.2.2. Effect of material selection in the SG dye removal by photodegradation and adsorption

It is important to stress that the choice between a raw material and a calcined material in a Fenton or photo-Fenton photodegradation reaction must be based on preliminary tests that may be necessary to evaluate the degradation efficiency of contaminants with each type of material, or prior knowledge of material properties and their interaction with contaminants.

For this purpose, calcining a material can modify its physico-chemical properties, including specific surface area, porosity and chemical composition. In some cases, calcination can improve the catalytic activity of the material by increasing the active surface area or modifying the distribution of active sites. So, if the calcined material has better catalytic activity, it may be preferable to use it in the photodegradation reaction.

The catalyst to be studied is the iron ore waste coming from EL OUENZA located in the willaya of Tébessa approximately 250 km from the iron and steel complex of ELHADJAR.

The material was ground and calcined to form the crystalline and active phases. Two tests were performed on the raw and calcined material to select the best-performing one. The results obtained are recorded in Fig. 4.

Fig. 4 shows the difference between the two catalysts, raw and calcined with sulfite as an oxidizing agent at pH = 3 under solar light. The degradation reaction was carried out for a period of 3 h.

According to Fig. 4, the crude catalyst gives a degradation rate of 3 %, however, the calcined catalyst gives a very efficient yield of 25 %. According to this result, the calcined catalyst was chosen for the continuation of our study.

Before any photocatalytic study, the adsorption kinetics of the dye on the catalyst must be established. This last one will occur in conditions of room temperature, at an initial concentration of pollutant equal to 10 mg L^{-1}, an initial pH of the solution equal to 3 and at 0.1 g L^{-1} of catalyst dose. The adsorption experiment was performed in the dark. The results obtained are shown in Fig. S1, which shows a slight decrease or a negligible change in the adsorption (<2 %) of SG in calcined powder of mining waste as a function of time.

Fig. 5 reveals that this material has poor adsorption capacity and it can be attributed to the repulsion phenom between the surface charge of mining waste powder and anionic SG dye molecules [67]. The obtained result revealed that the adsorption step is not significant. Hence, the adsorption step in the other experiments was eliminated.

3.3. The parametrical study of SG degradation and mineralization by heterogeneous photo Fenton process

This study of the classical photo-Fenton process involves optimizing the various parameters influencing the efficiency of the photo-Fenton reaction. The foremost parameters to be studied are the hydrogen peroxide concentration (H_2O_2) and ferrous ions (Fe^{2+}) concentrations, solution pH, reaction time and light intensity. Consequently, results and optimum conditions may vary according to the pollutant to be treated and the nature of the system studied.

3.3.1. Effect of catalyst loading

It is worth noting that the increasing of catalyst concentration can generally increase photocatalytic activity by providing more active sites for photoinduced reactions. This can lead to greater electron-hole pair generation and increased pollutant degradation efficiency [68].

The catalyst mass is an important factor that can have a big impact on the photodegradation process. Hence, it is necessary to select an optimal catalyst mass for particular applications, taking into account elements like practicality, degradation efficiency, reaction rate, light absorption, and scattering effects.

Several works in the literature have shown that a high concentration of the catalyst, especially Fe^{+2} in the solution, is not in favor of a better degradation rate [69]. This decrease in efficiency is due to the parasitic reaction between OH^- and Fe^{+2} [70]. Iron mining

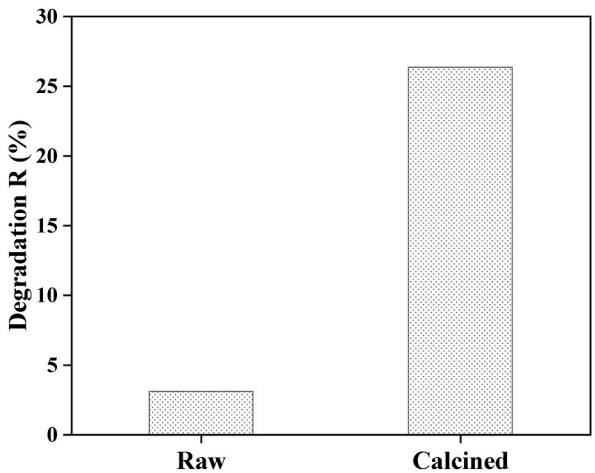

Fig. 4. Degradation rate of SG dye by crude and calcined form catalyst. P = 10 ppm, $m_{catalyst}$ = 0.1 g L^{-1}, $[Sulfite]_o$ = 0.15 mM, pH = 3 and for 180 min.

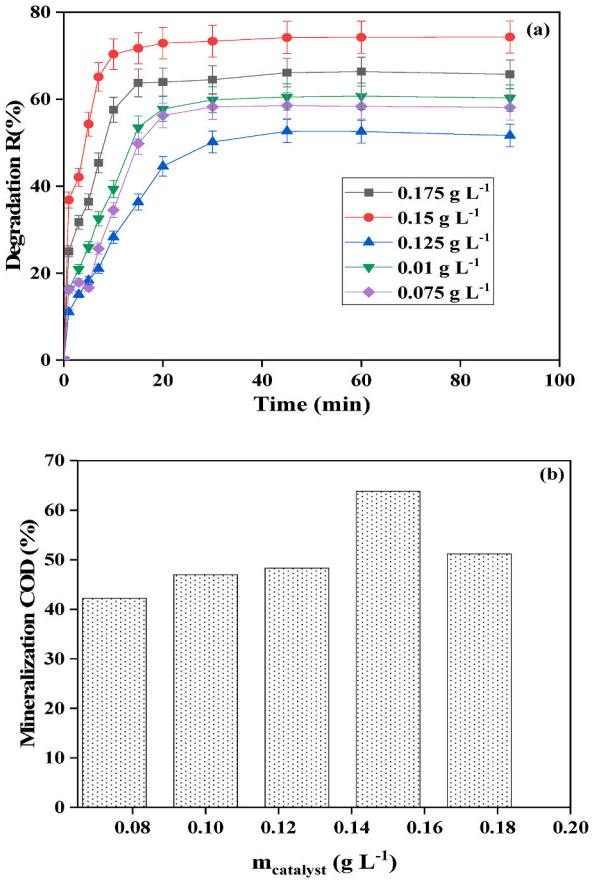

Fig. 5. Evolution of heterogeneous photo Fenton process as a function of different catalyst concentrations. [p]o = 10 mg L^{-1}, [Sulfite]o = 0.15 mM and pH = 3. a) rate of degradation, **b)** rate of mineralization of SG dye.

waste, used for the decontamination of wastewater, can be recovered and reused, as they are practically insoluble in water. Being widespread in soils, they can also be used for in-situ decontamination of soils and groundwater by injecting sulfite as an oxidizing agent [49,71].

To evaluate the optimal catalyst concentration, we varied the catalyst mass from 0.075 to 0.175 g L^{-1}, setting the sulfite oxidant concentration at 0.15 mM and the SG dye concentration at 10 mg L^{-1} in a medium with a pH of 3. The results of degradation and mineralization obtained are shown in Fig. 5.

The results obtained demonstrate that when increasing the catalyst concentration from 0.075 to 0.175 g L^{-1} for a reaction time of 90 min, the photodegradation rate increases from 57 % to 71 % and the COD removal rate increases from 42 to 63 %. For a concentration of catalyst higher than 0.075 g L^{-1}, we notice that the rate of degradation and mineralization are at maximum values of 71 % and 63.83 %, respectively, for a quantity of catalyst of 0.15 g L^{-1}. This result can be explained by the high number of active sites available which consequently facilitated and favored the contact with oxidant agents, leading to promote the photodegradation efficiency and the rate of reaction. However, the high amount of catalyst contributes to the low photodegradation activity because low penetration of solar energy to the site of the solid particles, hence the insufficient total number of photons being reactive with H_2O_2 molecules [72,73]. From the obtained result, the optimum dosage of the catalyst is chosen as 0.15 g L^{-1}.

3.3.2. Effect of sodium sulfite

Sodium sulfite plays a role as an oxidant and it can potentially affect the photodegradation mechanisms of certain compounds. For example, it can lead to changes in the pH of the solution. Furthermore, it may act as a sacrificial electron donor, participating in photochemical reactions that alter the photodegradation pathways of the target compound [74].

In order to understand the effect of the sulfite oxidant Na_2SO_3 concentration on the photo Fenton reaction, the concentration of calcined mining catalyst was fixed at 0.15 g L^{-1}, the concentration of sodium sulfite varied from 0.15 to 0.75 mM for a pH value of 3, and concentration SG dye was fixed at 10 mg L^{-1}. The evolutions of degradation and mineralization rates as a function of Na_2SO_3 concentration during the reaction tile are illustrated in Fig. 6.

From the results shown in Fig. 6(a and b), varying the concentration of Na_2SO_3 from 0.15 to 0.75 mM gives an increase in degradation rates from 45 % up to 90 % for 90 min of reaction. For a concentration of Na_2SO_3 higher than the value of 0.3 mM, the

degradation and mineralization rates increased and reached values of 92 % and 91.5 %, respectively, obtained with a concentration of 0.45 mM Na_2SO_3. The concentrations of 0.6 and 0.75 mM of sodium sulfite give a result almost similar to that of 0.45 mM. Thus, the degradation rate reaches the maximum for an optimum Na_2SO_3 concentration of 0.45 mM.

Sulfite radical is an active species with significant reducing and oxidizing capabilities via sulfate anions reacting with transition metal ions and can be applied effectively for the degradation of organic substances by other radicals [75–77].

The different reactions can be explained by a possible mechanism that sulfite anions react with photo-induced holes or hydroxyl radicals to produce sulfite radicals that attack organic molecules. There are two possible routes for the formation of sulfite radicals. Firstly, sulfite anions are oxidized directly by photo-induced holes at the valence band h_{VB} via the following reaction:

$$h + {}_{VB} + SO_3^{2-} \; SO_3{}^{*-} \tag{4}$$

The second way to produce sulfite radicals is for sulfite anions to react with hydroxyl radicals (OH^-).

$$h + {}_{VB} + H2O \; {}^*OH + H+ \tag{5}$$

$$^*OH + SO_3{}^{*-} \; SO_3{}^{*-} + OH^- \tag{6}$$

3.3.3. *Effect of pH*

The pH is considered a very important parameter in the photo-Fenton processes, because the pH affects and controls the rate of production in the concentration of hydroxyl radicals as well as the nature of the iron species in the solution. Adjusting the pH in the acidic zone is an essential step in the Fenton reaction [78].

To investigate the pH effect on the photo-Fenton degradation of SG dye, the experiments were carried out by varying the pH from 3 to 9, at a concentration of 0.45 mM of Na_2SO_3, the mass of catalyst at 0.15 g L^{-1}, and initial SG dye concentration at 10 mg L^{-1}. The results of this investigation are given in Fig. 7.

The previous figures show that the favorable pH for a better degradation rate of the SG dye by the photo Fenton process is a pH

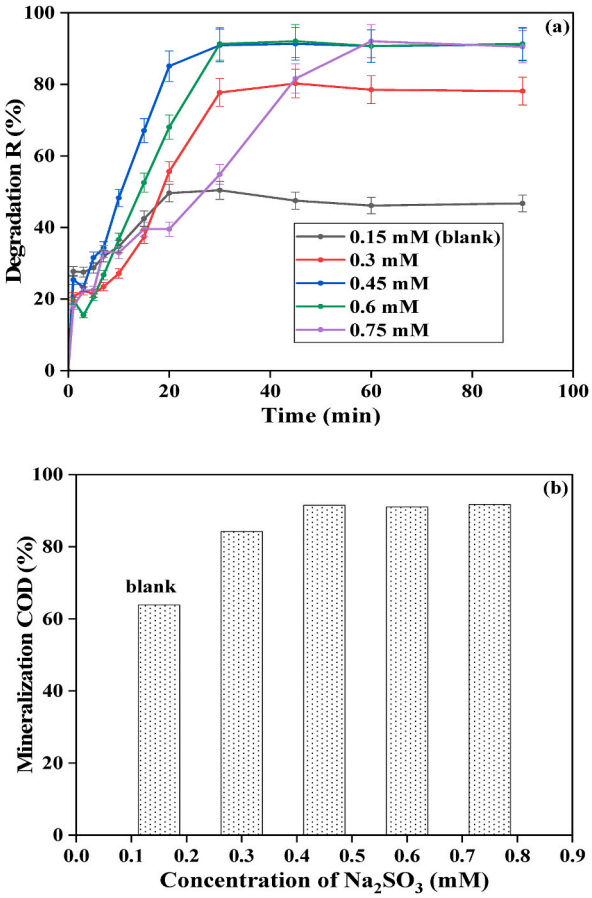

Fig. 6. Evolution of heterogeneous photo Fenton process as a function of different sulfite concentrations. $m_{catalyst}$ = 0.15 g L^{-1}, pH = 3 and [p]o = 10 mg L^{-1}. **a)** rate of degradation, **b)** rate of mineralization of SG dye.

equal to 3, with a yield of 90 % and after 90 min. As shown in Fig. 7, for a pH value of around 3, it was found that the H_2O_2 decomposition within hydroxyl radicals production was enhanced. Thus, the availability of many free radicals enables water decomposition and promotes dye degradation. These results are in good agreement with those already observed in the study of the degradation of different dyes by the Fenton process [79].

3.4. The parametrical study of SG dye degradation and mineralization by modified heterogeneous photo Fenton process

To boost the photodegradation and mineralization of organic contaminants, the modified heterogeneous photocatalytic Fenton process combines the principles of heterogeneous photocatalysis with Fenton chemistry. Because most of the available technologies of water treatment are inadequate for reducing some pollutants, the development and research of eco-technologies for water treatment are in constant evolution. As a modification of conventional water treatment processes, photo Fenton consists of enhancing the generation of reactive hydroxyl radical *OH, in order to oxidize and degrade organic contaminants, modification of the heterogeneous photo Fenton process with the aim of achieving complete conversion of the organic pollutants into carbon dioxide (CO_2) and water (H_2O) with high efficiency and in a short time has been investigated.

From the previous study, it was found that the homogeneous process involving Fe^{3+}/Ligand and Fe^{2+}/Ligand complexes dominated the mineralization of organic pollutants when the total dissolved iron concentration reached a high level. However, a drawback of the leaching of iron still remains. In fact, the iron in the homogeneous system will regenerate and remain in solution according to the following equations:

$$Fe^{3+} + O_2^{\bullet -} \rightarrow Fe^{2+} + O_2 \quad (7)$$

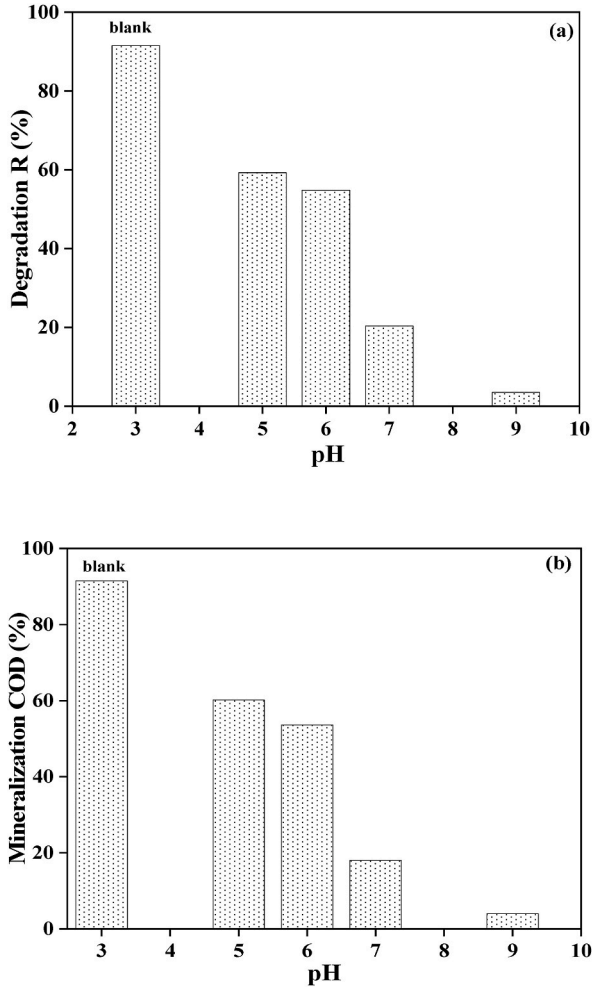

Fig. 7. Evolution of heterogeneous photo Fenton process as a function of different pH, [P]o = 10 mg L^{-1}, m $_{catalyst}$ = 0.15 g L^{-1} and [Sulfite]o = 0.45 mM. **a)** rate of degradation, **b)** rate of mineralization of SG dye.

$$Fe^{3+} + H.O._2^{\bullet -} \rightarrow Fe^{2+} + O_2 \quad (8)$$

$$Fe^{2+} + O_2^{\bullet -} \rightarrow Fe^{3+} + H_2O_2 \quad (9)$$

$$Fe^{2+} + H.O._2^{\bullet -} \rightarrow Fe^{3+} + H_2O_2 \quad (10)$$

Another improved method is to regulate the catalytic process. Thus, the ideal catalytic process should take full advantage of homogeneous reactions for the degradation of organic pollutants and heterogeneous catalysts for reuse after treatment. Over the last two decades, some research has focused on the effect of carboxylate ligands on the photochemical degradation of organic contaminants. It has been reported that carboxylate ligands, including citrate, malonate, oxalate and tartrate, have a different impact on the quantum yield of Fe^{2+} in a homogeneous photochemical system [45,80]. Moreover, in the heterogeneous photodegradation system, oxalate positively impacted the degradation process of organic contaminants and expanded the range of the solar spectrum up to 450 nm [81].

In this part of our work, studying the heterogeneous photo Fenton process enhanced by oxalate will bring better insight into understanding the mechanism involved between the carboxylate ligands and the catalytic activity of iron oxides in our system. However, to identify the performance of the process, it is necessary to evaluate the influence of ligand concentration and other operating parameters such as the catalyst dose, pH of the solution, Na_2SO_3 concentration, and the SG dye concentration.

3.4.1. *Effect of catalyst loading*

The effect of the amount of catalyst is evaluated by applying varied mass of catalyst from 0.075 to 0.175 g L^{-1} while maintaining the other experimental conditions fixed as complex concentration $[Lig]_o = 0.1$ mM, dye concentration at 10 mg L^{-1} and unadjusted pH solution. The obtained results are presented in Fig. 8.

Fig. 8(a) shows that the increase in iron ore concentration always leads to an increase in the reaction rate of photodegradation. Nevertheless, according to the obtained result, a delay of decolorization with increasing iron catalyst was observed. This can be due to blocking light penetration to reach the maximum active site on the iron catalyst surface.

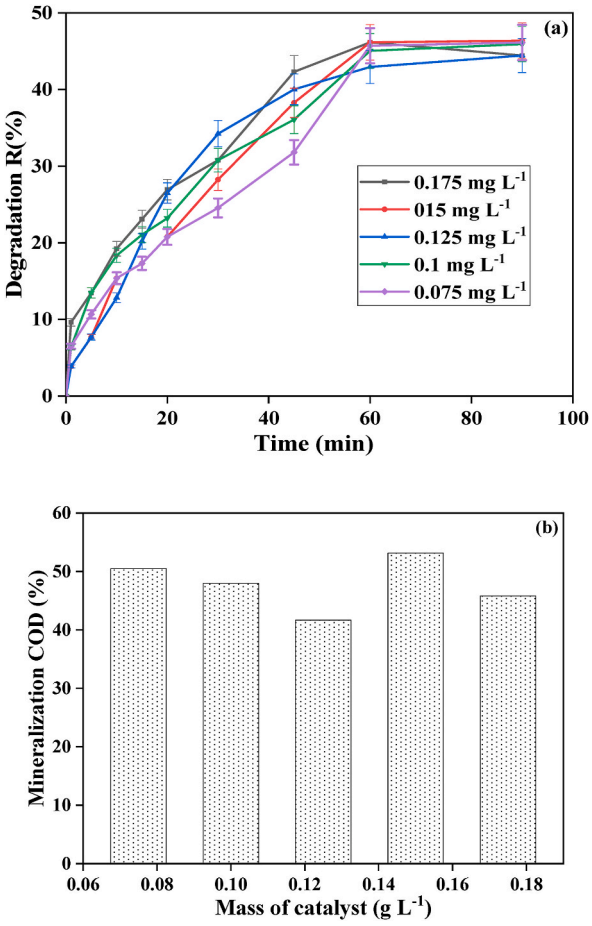

Fig. 8. Evolution of modified heterogeneous photo Fenton process as a function of different ore concentrations, $[P]_o = 10$ mg L^{-1}, $[Lig]_o = 0.1$ mM and unadjusted pHi. **a)** rate of degradation, **b)** rate of mineralization of SG dye.

From the obtained results, it is observed that an increase in the catalyst concentration has allowed for delaying the decoloration reaction. This can be explained by the screening effects due to the aggregation of the catalyst particles that prevents photons from reaching the maximum of the catalyst surface. The maximum degradation and mineralization rates are 49.23 % and 50.5 % respectively. An increase in the iron ore concentration beyond the concentration necessary to absorb all the photons inside the photo reactor still leads to an increase in the reaction rate [49].

3.4.2. *Effect of oxalic acid*

Real effluents can be complex and contain various chemical compounds, pollutants, and impurities from different origins of household, agricultural and industrial contamination. They also frequently contain chelating agents, such as detergents, stabilizers, and metal ion masking agents, which can inhibit the advanced iron-based oxidation process (Fe^{2+}/Fe^{3+}) by masking the impact of chelating agents on the Fenton and photo-Fenton reaction. Several chelating agents for iron and transition metals have been reported in the literature, such as oxalic acid, citric acid, Ethylenediamine-N, N-disuccinic acid, EDTA and Nitrilotriacetic acid [82].

Overall, it is well known that the addition of oxalic acid is a beneficial strategy for improving the performance of the Photo-Fenton reaction, preventing the precipitation of Fe^{2+}/Fe^{3+}, making photocatalytic sewage treatment more effective and versatile for wastewater treatment and micropollutant degradation [83–85]. Therefore, optimizing the concentration of oxalic acid is essential to achieve the desired degradation efficiency. Different concentrations (0.1–0.3 mM) of this Ligand were tested while keeping the other parameters constant to highlight the oxalic acid concentration effect. The experimental results reported in the following Fig. 9 (a, b) allow us to compare the photo-Fenton degradation curves of the SG dye at different oxalic acid concentrations.

From the results shown in Fig. 9(a), it appears that the best efficiency is obtained at 0.25 mmol. L^{-1}. The initial rate of reaction deduced from the curves show that the rate of disappearance is about 3 times greater by going from 10^{-4} to 5×10^{-4} mmol. L^{-1}. It is well known that when oxalic acid is added to the photo-Fenton reaction, oxalate acts both as an electron donor and as a surface complexing agent for iron ions Fe(II) or Fe(III), forming iron-oxalate complexes that promote the detachment of metal centers from the surface and expanding the solar radiation spectrum range absorption [86].

In addition, oxalic acid also functions as a chelating agent, which keeps iron ions in solution and stops them from forming iron hydroxides as a result of precipitation above of pH 2.8. This suppresses the oxalic acid/H_2O_2 combination. As a result of improved

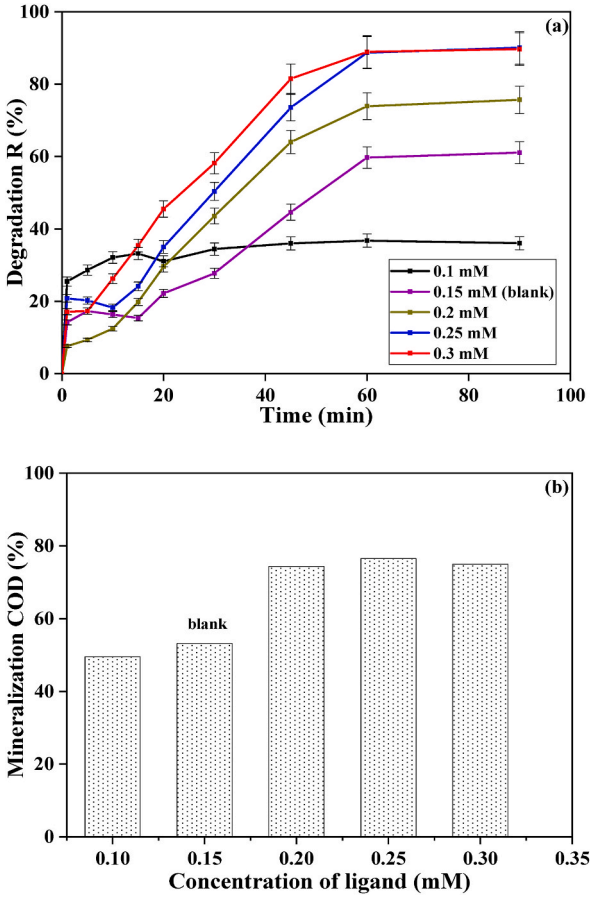

Fig. 9. Evolution of modified heterogeneous photo Fenton process as a function of different oxalic acid concentrations, $m_{catalyst} = 0.075$ g L^{-1}, [P]o = 10 mg L^{-1} and pHi not adjusted. **a)** rate of degradation, **b)** rate of mineralization of SG dye.

interaction between the catalyst and the organic contaminants and the maintenance of a uniform reaction mixture, degradation efficiency is increased [87,88]. The optimal mass of oxalic acid chosen for the rest of the study is 0.25 mM.

3.4.3. *Effect of the concentration of sodium sulfite*

Overall, the studies suggest that the effect of Na_2SO_3 concentration on the degradation photo Fenton reaction may vary depending on the reaction conditions. However, low concentrations of Na_2SO_3 can be used to promote the degradation of organic compounds.

To enhance the photodegradation of 10 mg L^{-1} of SG dye, the study of the effect was performed with different values of Na_2SO_3 concentration during solar irradiation at free solution pH, a catalyst mass of 0.075 g L^{-1} and an oxalic acid concentration of 0.25 mM. The results are given in Fig. 10.

In the case of SG dye degradation, when the sodium sulfate concentration is increased from 0.3 to 0.75 mM, the degradation rate increases slightly as shown in Fig. 10(a). The rate of degradation increases with increasing sodium sulfate concentration up to 0.3 mM. An excess sulfate ions react with water molecules, resulting in the generation of hydroxyl radicals, as shown in Fig. 10.

The results presented in Fig. 10 (a, b) show that the increase in the oxidizing agent concentration is accompanied by a slight acceleration of the rate of discoloration. This demonstrates that, in order to accomplish the electro-transfer process, the decomposition of SO_3^{2-} ions serves as a hole scavenger that leads to the production of $*SO_3^-$ radicals [89]. Iron mining waste (hematite phase α-Fe_2O_3) can produce photogenerated electrons (e^-) in the conduction band and holes (h^+) in the valence band when it is exposed to radiation. The (e^-) reacts with O_2 to make $*O_2^-$, which then produces $*HO_2$ and OH*. The (h^+) mixes with H_2O to give *OH. Furthermore, (e^-) can participate in the *OH formation by reacting with H_2O_2 to produce OH*, which in turn reduces Fe^{+3} to Fe^{2+} on the hematite surface.

Additionally, carboxylic acid (oxalic acid) Fe^{3+}—oxalate can be rapidly reduced to Fe^{2+}—oxalate under radiation, forming $*C_2O_4^-$ radicals. Moreover, OH* can be produced via the reaction of Fe^{2+}—oxalate with H_2O_2. This explains why adding oxalic acid increased the degrading efficiency of the photo-Fenton system.

In contrast to the mineralization where their rate exhibits a gradual and minimal rate of change, the addition of the oxidant sulfite does not attribute any case on the significant improvement of the photodegradation process that can be due to the fact that the ligand reacts more quickly with the catalyst than the catalyst with the sulfite, then the sulfite remains in solution serving as an inhibiting agent

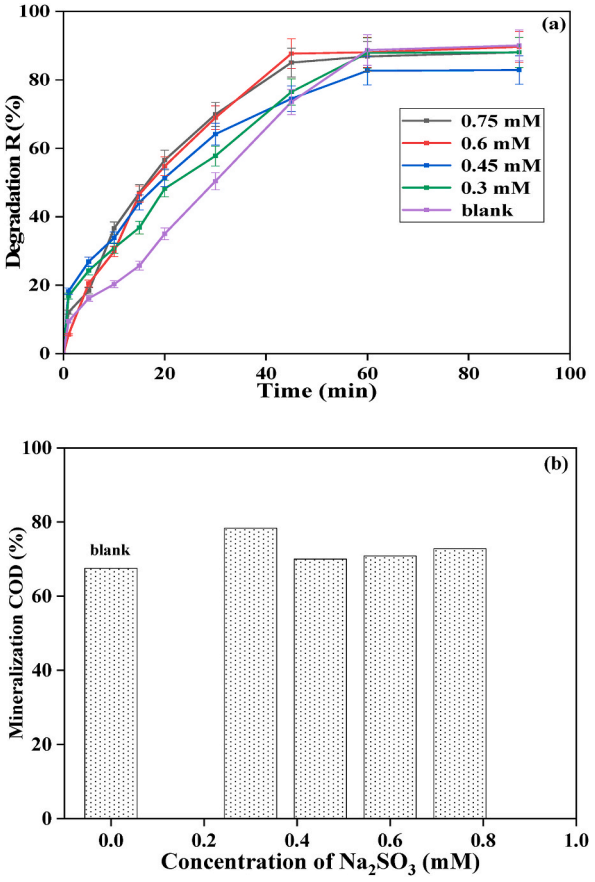

Fig. 10. Evolution of modified heterogeneous photo Fenton process as a function of different concentrations of Na_2SO_3, at unadjusted pH, [P]o = 10 mg L^{-1}, $m_{catalyst}$ = 0.015 g L^{-1} and [Lig]o = 0.25 mM. **a)** rate of degradation, **b)** rate of mineralization of SG dye.

and allowing competition between the pollutant and the sulfite with the radicals released in solution [90].

3.4.4. Effect of the pH

Given the substantial impact on the degradation of organic compounds employing photo Fenton methods, the pH parameter must be considered while optimizing photodegradation reactions.

Further studies have shown that the pH variations affect the reactivity of the reactants (Fe^{2+}, Fe^{3+}, oxidant). Hence, this parameter significantly influences the concentration of species in the solution, leading to the formation of iron complexes and affecting the reaction of photo Fenton [91]. At lower pH between 1 and 2, oxalic acid exists mainly in the $H_2C_2O_4$ form, while $HC_2O_4^-$ is the most predominant species at pH 2.5–3.0. However, with pH above 4, $C_2O_4^{-2}$ is the dominant species [89]. Therefore, the effect of pH was investigated through a series of experiments with pH values changing from 2 to 8, the initial concentration solution of the SG dye fixed at 10 mg L^{-1}, the concentration of ligand at 0.25 mM, and the mass of catalyst at 0.075 g L^{-1}. The obtained results of this study are given in Fig. 11(a and b).

Fig. 11(a, b) shows that SG dye degradation is related to different pH values after 90 min of irradiation under sunlight and it can be noticed that the best degradation and mineralization rates are 82 % and 78.5 %, respectively, and are obtained at fixed pH values. This behavior is due to the reactivity of the ligand in the acid medium. For pH values below neutrality, oxalate ions predominate. The latter form surface complexes on the iron ore, which decompose under the effect of light by generating radical species, leading to a better efficiency of the modified photo Fenton process [92].

The rate of degradation and mineralization removal efficiency are lower for acidic pH = 2 and this can be due to the iron leached at low pH or because of the interaction of hydroxyl radicals and H_2O_2 with H^+ and also the reduced concentration of hydroxyl radicals [93].

Moreover, the low rates of degradation and mineralization obtained at high pH values up to 6 can be attributed to the low photoactivity of those soluble iron-organic pollution complexes, which lead to highly alkaline conditions for the inhibition of active species [94,95]. Finally, these results suggest that the choice of catalyst, which in our case is calcined mine waste products, has enabled us to use the heterogeneous photo Fenton reaction over a wide range of pH values for the efficient catalytic degradation of contaminants.

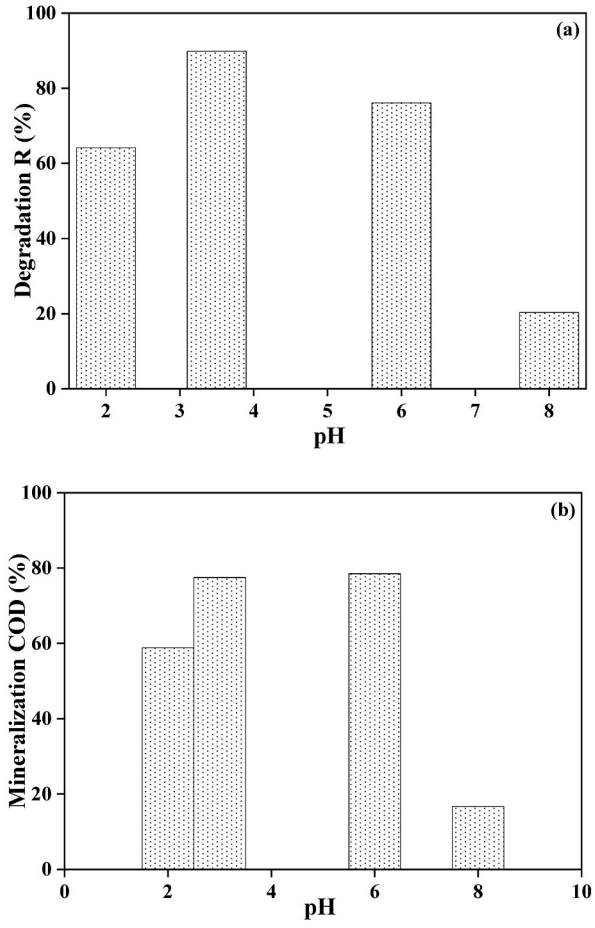

Fig. 11. Evolution of modified heterogeneous photo Fenton process as a function of different pH, [P]o = 10 mg L^{-1}, $m_{catalyst}$ = 0.015 g L^{-1} and [Lig]o = 0.25 mM. **a)** rate of degradation, **b)** rate of mineralization of SG dye.

3.4.5. Effect of scavengers

The photo-Fenton degradation of various aquatic organic pollutants is carried out by primary reactive radical species generated in the hematite α-Fe_2O_3-based photo-Fenton System. These can be identified separately by introducing radical scavengers. To understand the scavenging mechanism, the photo-Fenton degradation of SG was performed utilizing isopropanol and chloroform with a concentration of 1 M for quenching hydroxyl radicals *OH and superoxide radicals $*O_2^-$, respectively. The obtained results are given in Fig. 12.

From Fig. 12, it can be observed that the degradation efficiency is significantly impacted by adding scavengers and the obtained values are reduced in the presence of this later separately or in the mixture (90.40 %). This phenomenon can be explained by the role of scavengers at quenching the reactive species [96,97]. In particular, the dye degradation removal efficiency in the presence of isopropanol decreased to 41.82 %, indicating that the *OH could be the most prevalent active oxygen. Furthermore, the chloroform gives a degradation efficiency of 68.5 % suggesting that $*O_2$ contributes minimally to the degradation of SG dye. However, adding a mixture of isopropanol and chloroform gives a degradation efficiency of 46.6 %, which is higher than that achieved with isopropanol alone. Additionally, the role of oxalate and (h^+) produced in the valence band of hematite should not be ignored [98].

3.5. Kinetic study of degradation and mineralization

The kinetic study of the modified heterogeneous photo-Fenton as a complex mechanism involves evaluating and characterizing reaction rates and understanding the reaction mechanisms that occur during the pollutant degradation reaction. For this purpose, experimental data can be analyzed using appropriate models that describe the modified photo-Fenton reaction to determine kinetic constants and the reaction to study reaction mechanisms.

Moreover, in most cases, the kinetics of degradation of many organic molecules by photo Fenton, are defined as first-order kinetics [99] or second-order kinetics reactions. The first-order kinetics is given by the following equation:

$$\frac{dC_t}{dt} = -k_1 C_t \tag{11}$$

And thus,

$$-ln\frac{C_t}{C_o} = k_1\, t \tag{12}$$

Here, t is time (min), k_1 is the first-order kinetic constant (min^{-1}), and C_t and C_o are the concentrations of SG dye at time t and the initial time (min).

For second-order reaction kinetics, the following can be obtained.

$$\frac{1}{C_t} = \frac{1}{C_o} - k_2\, t \tag{13}$$

Where k_2 is the kinetic rate constant of second-order reaction kinetic ($L.mg^{-1}\ min^{-1}$).

The half-time of SG photo-Fenton degradation for the first and second order reactions can be given by the following equations, respectively [100]:

$$t_{1/2} = \frac{0.693}{k1} \tag{14}$$

$$t_{1/2} = \frac{1}{k2 * Co} \tag{15}$$

The degradation and mineralization kinetics most appropriate for SG dye elimination were assessed by plotting the linear form of the first and second-order model equations (12) and (13). The parameters of kinetic, as well as the regression coefficients (R^2) and the half-life $t_{1/2}$ for each reaction order were investigated. The obtained results are given in Table 3.

In order to determine the order of the degradation reaction of the modified photo Fenton process, the first and second-order kinetic models were fitted to data from experiments carried out with 0.25 mM in ligand and 0.075 g L^{-1} in catalyst mass and an unadjusted pH.

The results are summarized in Table 3.

Examining the results in Table 3 reveals that the kinetic study of the reaction is well-fitted to a first-order reaction. We note that the R^2 of 0.9862 and a rate constant k = 0.0233 L $mol^{-1}.S^{-1}$ for the degradation and R^2 of 0.8603 and a K = 0.0326 L $mol^{-1}.S^{-1}$ for the mineralization, these results indicate that the first order kinetic model is more adequate for the description of our experimental results [53].

Moreover, another critical kinetic indication is $t_{1/2}$ (the half-life of a process), which corresponds to the time taken for the dye concentration decreasing by half. The examination of their value in Table 3 revealed that the calculated $t_{1/2}$ is a function of the nature of the photo Fenton reaction and it is significant in the case of Fe(III)/ligan complex.

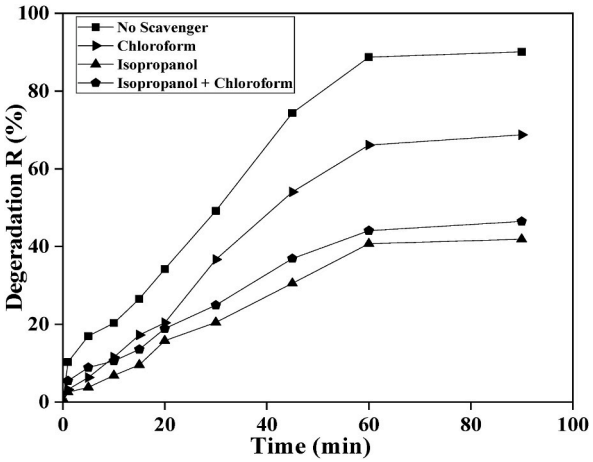

Fig. 12. Effect of various scavengers on the degradation of SG dye in the modified heterogenous photo-Fenton reaction under sunlight, pH = 6, $m_{catalyst}$ = 0.015 mg L^{-1}, Lig_o = 0.25 M, [P]o = 10 mg/L.

Table 3
Analysis of the kinetic models applied for the two-process heterogeneous photo Fenton and modified heterogeneous photo-Fenton for SG Removal.

Concentration mM	Degradation						Mineralization					
	First order			Second order			First order			Second order		
	k_1	$t_{1/2}$ (S)	R^2	k_2	$t_{1/2}$ (S)	R^2	k_1	$t_{1/2}$ (S)	R^2	k_2	$t_{1/2}$ (S)	R^2
0.1	0.0218	31.78	0.959	0.054	185.18	0.2096	0.0062	111.77	0.899	0.0105	952.38	0.5748
0.15	0.0094	73.72	0.964	0.0197	338.40	0.8409	0.0241	28.75	0.8581	0.0492	135.50	0.6696
0.2	0.0238	29.11	0.9982	0.0882	56.68	0.9341	0.0197	35.17	0.9854	0.0507	98.62	0.5496
0.25	0.0233	29.74	0.9862	0.1034	38.68	0.8393	0.0326	21.25	0.8603	0.0357	112.04	0.3174
0.3	0.0358	19.35	0.9791	0.1663	20.04	0.842	0.0168	41.25	0.9528	0.0508	65.62	0.6637

3.6. *Proposed modified heterogeneous photo Fenton mechanism*

The proposed mechanistic study is shown in Fig. 13, which illustrates degradation and mineralization with the classic and modified heterogeneous photo Fenton of the SG dye molecule in the presence of the catalyzer from heat-treated iron ore waste (Fe_2O_3) and under sunlight in the presence of the following reagents H_2O_2, Na_2SO_3, oxalic acid, sodium sulfite. Knowing that this is a very complex mechanism, Fig. 13 shows the intervention of several elements in the degradation and mineralization reaction such as electrons e^-,

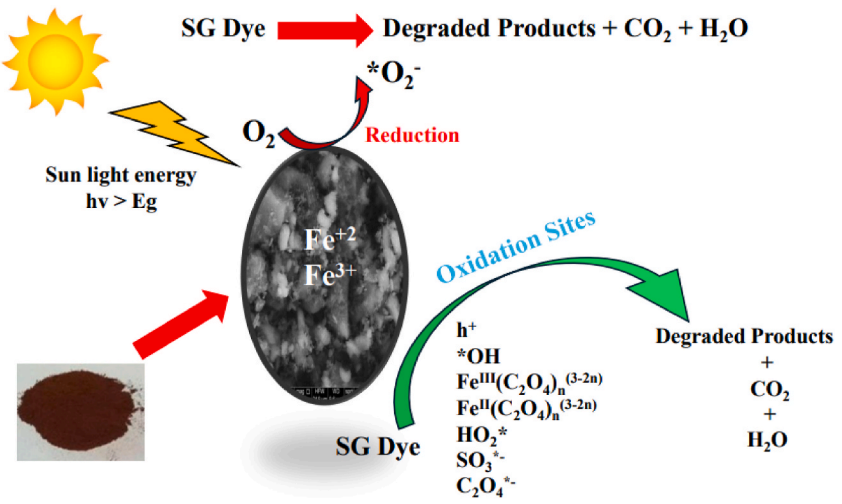

Fig. 13. Schematic illustration of the sunlight heterogeneous photo Fenton and the modified heterogeneous photo Fenton for the degradation and mineralization of SG dye.

Fe^{3+} and various oxidizing radicals such as h^+ holes, hydroxyl radicals *OH, $H_2O_2^-$*, HO_2*, SO_3^{*-}, $C_2O_4^-$* superoxide radicals $*O_2^-$, Ferri/ferrous-oxalate complexes $Fe^{3+}(C_2O_4)_n^{(3-2n)}$ and $Fe^{2+}(C_2O_4)_n^{(3-2n)}$.

These radicals are generated on the surface of the solid catalyst, with charge transfer from the Fe^{3+} based ligand of the iron oxide/oxalate complex, and play a key role in the photo Fenton degradation and mineralization activity of SG dye [80]. This approach of using solid iron oxide provides an alternative source of iron and leads to good separation of photogenerated carriers.

4. Conclusion

This study pursued two principal objectives. Firstly, the successful mechanical and thermal preparation of a catalyst powder rich in α-Fe_2O_3 hematite through the valorization of the El Ouenza iron ore mine waste and their physicochemical characterizations. Secondly, the prepared catalyst was effectively used in advanced heterogeneous photo Fenton and modified heterogeneous photo Fenton oxidation processes for the degradation and mineralization of SG food dye under sunlight illumination. Notably, the results of the parametric study of the modified photo Fenton process revealed a maximum degradation and mineralization rate of 90 % and 77.5 %, respectively, obtained with a ligand concentration of 0.25 mM, a catalyst dose of 0.15 g L^{-1} and an unadjusted pH. Additionally, because of the rapid reaction of the ligand with the α-Fe_2O_3 catalyst or the need for concentration prudence in the photodegradation process, the oxidant sulfite does not greatly improve the photodegradation efficiency. Also, kinetic studies revealed that the photo-Fenton degradation and mineralization process followed a first-order kinetic model. Moreover, the degradation mechanism of SG involved the formation of reactive oxygen species (ROS), such as hydroxyl radicals and superoxide radicals. Furthermore, holes (h^+) generated after α-Fe_2O_3 irradiation and the $C_2O_4^{*-}$ ferrioxalate radical significantly contributed to the excellent photocatalytic performances in the heterogenous photo-Fenton process. Consequently, the study reveals that a naturally prepared iron mining waste catalyst has low pH dependence, enabling near-neutral water treatment under sunlight irradiation as a sustainable green energy. This heterogeneous modified photo Fenton process eliminates acidification and chemical reagent consumption, reducing the salt load in treated water. This finding has great potential for use in efficient environmental wastewater cleanup applications.

CRediT authorship contribution statement

Mohammed Kebir: Writing – original draft, Visualization, Methodology, Investigation, Conceptualization. **Hichem Tahraoui:** Writing – review & editing, Writing – original draft, Investigation. **Imene Kahina Benramdane:** Formal analysis, Conceptualization. **Noureddine Nasrallah:** Supervision, Resources, Formal analysis. **Selma Toumi:** Writing – review & editing, Formal analysis, Conceptualization. **Jie Zhang:** Writing – review & editing, Visualization, Validation. **Abdeltif Amrane:** Writing – review & editing, Visualization, Validation, Supervision, Resources.

Declaration of competing interest

The authors declare that they have no known competing financial interests or personal relationships that could have appeared to influence the work reported in this paper.

Data availability

Data will be made available on request.

Acknowledgments

This work is financially supported by the Ministry of Higher Education and Scientific Research and the Directorate General for Scientific Research and Technological Development of Algeria.

Appendix A. Supplementary data

Supplementary data to this article can be found online at https://doi.org/10.1016/j.wri.2024.100269.

References

[1] H. Tahraoui, S. Toumi, M. Boudoukhani, N. Touzout, A.N.E.H. Sid, A. Amrane, A.-E. Belhadj, M. Hadjadj, Y. Laichi, M. Aboumustapha, Evaluating the effectiveness of coagulation–flocculation treatment using aluminum sulfate on a polluted surface water source: a year-long study, Water 16 (2024) 400.
[2] C. Djama, A. Bouguettoucha, D. Chebli, A. Amrane, H. Tahraoui, J. Zhang, L. Mouni, Experimental and theoretical study of methylene blue adsorption on a new raw material, cynara scolymus—a statistical physics assessment, Sustainability 15 (2023) 10364, https://doi.org/10.3390/su151310364.
[3] P. Chowdhary, R.N. Bharagava, S. Mishra, N. Khan, Role of industries in water scarcity and its adverse effects on environment and human health, Environ. Concerns Sustain. Dev. (2020) 235–256.

[4] H. Tahraoui, S. Toumi, A.H. Hassein-Bey, A. Bousselma, A.N.E.H. Sid, A.-E. Belhadj, Z. Triki, M. Kebir, A. Amrane, J. Zhang, Advancing water quality research: K-nearest neighbor coupled with the improved grey wolf optimizer algorithm model unveils new possibilities for dry residue prediction, Water 15 (2023) 2631.

[5] A. Hadadi, A. Imessaoudene, J.-C. Bollinger, A. Bouzaza, A. Amrane, H. Tahraoui, L. Mouni, Aleppo pine seeds (Pinus halepensis Mill.) as a promising novel green coagulant for the removal of Congo red dye: optimization via machine learning algorithm, J. Environ. Manag. 331 (2023) 117286.

[6] N. Bouchelkia, H. Tahraoui, A. Amrane, H. Belkacemi, J.-C. Bollinger, A. Bouzaza, A. Zoukel, J. Zhang, L. Mouni, Jujube stones based highly efficient activated carbon for methylene blue adsorption: kinetics and isotherms modeling, thermodynamics and mechanism study, optimization via response surface methodology and machine learning approaches, Process Saf. Environ. Protect. 170 (2023) 513–535.

[7] S. Farch, M.M. Yahoum, S. Toumi, H. Tahraoui, S. Lefnaoui, M. Kebir, M. Zamouche, A. Amrane, J. Zhang, A. Hadadi, Application of walnut shell biowaste as an inexpensive adsorbent for methylene blue dye: isotherms, kinetics, thermodynamics, and modeling, Separations 10 (2023) 60.

[8] A. Imessaoudene, S. Cheikh, A. Hadadi, N. Hamri, J.-C. Bollinger, A. Amrane, H. Tahraoui, A. Manseri, L. Mouni, Adsorption performance of zeolite for the removal of Congo red dye: factorial design experiments, kinetic, and equilibrium studies, Separations 10 (2023) 57.

[9] A. Singh, A. Roy, Fungal communities for the remediation of environmental pollutants, Recent Trends Mycol. Res. (2021) 127–165. Vol. 2 Environ. Ind. Perspect.

[10] R. Christie, Colour Chemistry, Royal society of chemistry, 2014.

[11] A. Gürses, M. Açıkyıldız, K. Güneş, M.S. Gürses, Dyes and Pigments, Springer, 2016.

[12] R. Anliker, G.C. Butler, E.A. Clarke, U. Förstner, W. Funke, C. Hyslop, G. Kaiser, C. Rappe, J. Russow, G. Tölg, Organic dyes and pigments, Anthropog. Compd. (1980) 181–215.

[13] D.M. Marmion, Handbook of US Colorants: Foods, Drugs, Cosmetics, and Medical Devices, John Wiley & Sons, 1992.

[14] S. Mechati, M. Zamouche, H. Tahraoui, O. Filali, S. Mazouz, I.N.E. Bouledjemer, S. Toumi, Z. Triki, A. Amrane, M. Kebir, Modeling and optimization of hybrid Fenton and ultrasound process for crystal violet degradation using AI techniques, Water 15 (2023) 4274.

[15] N. Hamri, A. Imessaoudene, A. Hadadi, S. Cheikh, A. Boukerroui, J.-C. Bollinger, A. Amrane, H. Tahraoui, H.N. Tran, A.O. Ezzat, Enhanced adsorption capacity of methylene blue dye onto kaolin through acid treatment: batch adsorption and machine learning studies, Water 16 (2024) 243.

[16] A. Kumar, U. Dixit, K. Singh, S.P. Gupta, M.S.J. Beg, Structure and properties of dyes and pigments, Dyes Pigments Nov. Appl. Waste Treat. (2021) 131.

[17] J.M. Navia-Mendoza, O.A.E. Filho, L.A. Zambrano-Intriago, N.R. Maddela, M.M.M.B. Duarte, L.S. Quiroz-Fernández, R.J. Baquerizo-Crespo, J.M. Rodríguez-Díaz, Advances in the application of nanocatalysts in photocatalytic processes for the treatment of food dyes: a review, Sustainability 13 (2021) 11676.

[18] A. Turner, Black plastics: linear and circular economies, hazardous additives and marine pollution, Environ. Int. 117 (2018) 308–318.

[19] K. Chan, Y. Leung Ng, E.K. Luk, Impact of celebrity endorsement in advertising on brand image among Chinese adolescents, Young Consum. 14 (2013) 167–179.

[20] M. Andriamanantena, Valorisation de la biodiversité et études ethnobotanique, phyto-chimique et toxicologique des plantes tinctoriales de Madagascar: applications dans le domaine des colorants naturels, La Réunion, 2020.

[21] T. Coultate, R.S. Blackburn, Food colorants: their past, present and future, Color. Technol. 134 (2018) 165–186.

[22] L.-L. Jiang, K. Li, D.-L. Yan, M.-F. Yang, L. Ma, L.-Z. Xie, Toxicity assessment of 4 azo dyes in zebrafish embryos, Int. J. Toxicol. 39 (2020) 115–123.

[23] H. Takabi, J.B. Joshi, G.-J. Ahn, Security and privacy challenges in cloud computing environments, IEEE Secur. Priv. 8 (2010) 24–31.

[24] T. Robinson, G. McMullan, R. Marchant, P. Nigam, Remediation of dyes in textile effluent: a critical review on current treatment technologies with a proposed alternative, Bioresour. Technol. 77 (2001) 247–255.

[25] C. Menard, F. Heraud, J.-L. Volatier, J.-C. Leblanc, Assessment of dietary exposure of nitrate and nitrite in France, Food Addit. Contam. 25 (2008) 971–988.

[26] A.K. Alsukaibi, Various approaches for the detoxification of toxic dyes in wastewater, Processes 10 (2022) 1968.

[27] M. Smara, R. Khalladi, N. Moulai-Mostefa, K. Madi, D. Mansour, S. Lekmine, O. Benslama, H. Tahraoui, J. Zhang, A. Amrane, Efficiency of hydrogen peroxide and Fenton reagent for polycyclic aromatic hydrocarbon degradation in contaminated soil: insights from experimental and predictive modeling, Processes 12 (2024) 621.

[28] K. Madi, D. Chebli, H. Ait Youcef, H. Tahraoui, A. Bouguettoucha, M. Kebir, J. Zhang, A. Amrane, Green fabrication of ZnO nanoparticles and ZnO/rGO nanocomposites from Algerian date syrup extract: synthesis, characterization, and augmented photocatalytic efficiency in methylene blue degradation, Catalysts 14 (2024) 62.

[29] M.I. Kanjal, M. Muneer, M.A. Jamal, T.H. Bokhari, A. Wahid, S. Ullah, A. Amrane, A. Hadadi, H. Tahraoui, L. Mouni, A study of treatment of reactive red 45 dye by advanced oxidation processes and toxicity evaluation using bioassays, Sustainability 15 (2023) 7256.

[30] H. Tahraoui, A.-E. Belhadj, Z. Triki, N.R. Boudellal, S. Seder, A. Amrane, J. Zhang, N. Moula, A. Tifoura, R. Ferhat, Mixed coagulant-flocculant optimization for pharmaceutical effluent pretreatment using response surface methodology and Gaussian process regression, Process Saf. Environ. Protect. 169 (2023) 909–927.

[31] R.P. Singh, P.K. Singh, R. Gupta, R.L. Singh, Treatment and recycling of wastewater from textile industry, Adv. Biol. Treat. Ind. Waste Water Their Recycl. Sustain. Future (2019) 225–266.

[32] M. Zamouche, M. Chermat, Z. Kermiche, H. Tahraoui, M. Kebir, J.-C. Bollinger, A. Amrane, L. Mouni, Predictive model based on K-nearest neighbor coupled with the gray wolf optimizer algorithm (KNN_GWO) for estimating the amount of phenol adsorption on powdered activated carbon, Water 15 (2023) 493.

[33] M. Gavrilescu, Environmental biotechnology: achievements, opportunities and challenges, Dyn. Biochem. Process Biotechnol. Mol. Biol. 4 (2010) 1–36.

[34] U.S.P. Uday, T.K. Bandyopadhyay, B. Bhunia, Bioremediation and Detoxification Technology for Treatment of Dye (S) from Textile Effluent, Text. Wastewater Treat, 2016, pp. 75–92.

[35] F.S.A. Khan, N.M. Mubarak, Y.H. Tan, M. Khalid, R.R. Karri, R. Walvekar, E.C. Abdullah, S. Nizamuddin, S.A. Mazari, A comprehensive review on magnetic carbon nanotubes and carbon nanotube-based buckypaper for removal of heavy metals and dyes, J. Hazard Mater. 413 (2021) 125375.

[36] U.I. Gaya, A.H. Abdullah, Heterogeneous photocatalytic degradation of organic contaminants over titanium dioxide: a review of fundamentals, progress and problems, J. Photochem. Photobiol. C Photochem. Rev. 9 (2008) 1–12.

[37] L. Zhang, S. Huo, W. Li, L. Song, W. Fu, J. Li, M. Gao, Improved heterogeneous photo-Fenton-like degradation of ofloxacin through polyvinylpyrrolidone modified CuFeO2 catalyst: performance, DFT calculation and mechanism, Sep. Purif. Technol. 311 (2023) 123261.

[38] N.I. Poshtiri, A.D. Koohi, A.E. Pirbazari, F.E.K. Saraei, Catalytic activity of magnetite fish-scales and tea-waste as heterogeneous photo-Fenton catalysts for removal of methyl orange through Cu (II) adsorption, Mater. Chem. Phys. 290 (2022) 126525.

[39] T.A.G. Martins, I.B.A. Falconi, G. Pavoski, V.T. de Moraes, M. dos, P.G. Baltazar, D.C.R. Espinosa, Green synthesis, characterization, and application of copper nanoparticles obtained from printed circuit boards to degrade mining surfactant by Fenton process, J. Environ. Chem. Eng. 9 (2021) 106576.

[40] A. Mashayekh-Salehi, K. Akbarmojeni, A. Roudbari, J.P. van der Hoek, R. Nabizadeh, M.H. Dehghani, K. Yaghmaeian, Use of mine waste for H2O2-assisted heterogeneous Fenton-like degradation of tetracycline by natural pyrite nanoparticles: catalyst characterization, degradation mechanism, operational parameters and cytotoxicity assessment, J. Clean. Prod. 291 (2021) 125235.

[41] M.A. Prada-Vásquez, S.E. Estrada-Flórez, E.A. Serna-Galvis, R.A. Torres-Palma, Developments in the intensification of photo-Fenton and ozonation-based processes for the removal of contaminants of emerging concern in Ibero-American countries, Sci. Total Environ. 765 (2021) 142699.

[42] Y. Pandey, A. Verma, A.P. Toor, Abatement of paraquat contaminated water using solar assisted heterogeneous photo-Fenton like treatment with iron-containing industrial wastes as catalysts, J. Environ. Manag. 325 (2023) 116550.

[43] I.N. Dias, B.S. Souza, J.H. Pereira, F.C. Moreira, M. Dezotti, R.A. Boaventura, V.J. Vilar, Enhancement of the photo-Fenton reaction at near neutral pH through the use of ferrioxalate complexes: a case study on trimethoprim and sulfamethoxazole antibiotics removal from aqueous solutions, Chem. Eng. J. 247 (2014) 302–313.

[44] J.H. Pereira, D.B. Queiros, A.C. Reis, O.C. Nunes, M.T. Borges, R.A. Boaventura, V.J. Vilar, Process enhancement at near neutral pH of a homogeneous photo-Fenton reaction using ferricarboxylate complexes: application to oxytetracycline degradation, Chem. Eng. J. 253 (2014) 217–228.

[45] H. Dai, S. Xu, J. Chen, X. Miao, J. Zhu, Oxalate enhanced degradation of Orange II in heterogeneous UV-Fenton system catalyzed by Fe3O4@ γ-Fe2O3 composite, Chemosphere 199 (2018) 147–153.
[46] L.O. Conte, G. Legnettino, D. Lorenzo, S. Cotillas, M. Prisciandaro, A. Santos, Degradation of Lindane by persulfate/ferrioxalate/solar light process: influential operating parameters, kinetic model and by-products, Appl. Catal. B Environ. 324 (2023) 122288.
[47] M.A.H. Karim, K.H.H. Aziz, K.M. Omer, Y.M. Salih, F. Mustafa, K.O. Rahman, Y. Mohammad, Degradation of aqueous organic dye pollutants by heterogeneous photo-assisted Fenton-like process using natural mineral activator: parameter optimization and degradation kinetics, in: IOP Conf. Ser. Earth Environ. Sci., IOP Publishing, 2021 012011.
[48] R.M. da Rocha Santana, D.C. Napoleão, J.M. Rodriguez-Diaz, R.K. de Mendonça Gomes, M.G. Silva, V.M.E. de Lima, A.A. de Melo Neto, G.M. Vinhas, M.M.M. B. Duarte, Efficient microbial cellulose/Fe3O4 nanocomposite for photocatalytic degradation by advanced oxidation process of textile dyes, Chemosphere 326 (2023) 138453.
[49] T. de Melo Augusto, P. Chagas, D.L. Sangiorge, T.C. de O. Mac Leod, L.C. Oliveira, C.S. de Castro, Iron ore tailings as catalysts for oxidation of the drug paracetamol and dyes by heterogeneous Fenton, J. Environ. Chem. Eng. 6 (2018) 6545–6553.
[50] R.D. Rios, I. Binatti, J.D. Ardisson, F.C. Moura, Compounds based on iron mining tailing dams and activated carbon from macauba palm for removal of emerging contaminants and phosphate from aqueous systems, Environ. Sci. Pollut. Res. 30 (2023) 60212–60224.
[51] C. De los Santos, H. Vidal, J.M. Gatica, M.P. Yeste, G. Cifredo, J. Castiglioni, Optimized preparation of washcoated clay honeycomb monoliths as support of manganese catalysts for acetone total combustion, Microporous Mesoporous Mater. 310 (2021) 110651.
[52] V.C. Farmer, The infrared spectra of minerals, Mineral. Soc. Monogr. 4 (1974) 331–363.
[53] M.M. Nour, M.A. Tony, H.A. Nabwey, Heterogeneous Fenton oxidation with natural clay for textile levafix dark blue dye removal from aqueous effluent, Appl. Sci. 13 (2023) 8948.
[54] T. Dippong, E.A. Levei, I. Petean, I.G. Deac, O. Cadar, A strategy for tuning the structure, morphology, and magnetic properties of MnFe2O4/SiO2 ceramic nanocomposites via mono-, di-, and trivalent metal ion doping and annealing, Nanomaterials 13 (2023) 2129.
[55] J. Madejova, P. Komadel, Baseline studies of the clay minerals society source clays: infrared methods, Clay Clay Miner. 49 (2001) 410–432.
[56] S.-B. Cho, J.-S. Noh, S.-J. Park, D.-Y. Lim, S.-H. Choi, Morphological control of Fe 3 O 4 particles via glycothermal process, J. Mater. Sci. 42 (2007) 4877–4886.
[57] F.B. Reig, J.G. Adelantado, M.M. Moreno, FTIR quantitative analysis of calcium carbonate (calcite) and silica (quartz) mixtures using the constant ratio method. Application to geological samples, Talanta 58 (2002) 811–821.
[58] H.A. Khalil, T.T. Ali Mahmoud, Direct formation of thermally stabilized amorphous mesoporous Fe2O3/SiO2 nanocomposites by hydrolysis of aqueous iron (III) nitrate in sols of spherical silica particles, Langmuir 24 (2008) 1037–1043.
[59] C.R. Nangah, T.G. Merlain, N.J. Nsami, C.P. Tubwoh, J. Foba-Tendo, K.J. Mbadcam, Synthesized goethite and natural iron oxide as effective absorbents for simultaneous removal of Co (II) and Ni (II) ions from water, J. Encapsulation Adsorpt. Sci. 9 (2019) 127.
[60] Y. Yamanoi, S. Nakashima, M. Katsura, Temperature dependence of reflectance spectra and color values of hematite by in situ, high-temperature visible micro-spectroscopy, Am. Mineral. 94 (2009) 90–97.
[61] M. Valášková, J. Tokarský, J. Pavlovský, T. Prostějovský, K. Kočí, α-Fe2O3 nanoparticles/vermiculite clay material: structural, optical and photocatalytic properties, Materials 12 (2019) 1880.
[62] S. Mohammadhosseini, T.J. Al-Musawi, R.M. Romero Parra, M. Qutob, M.A. Gatea, F. Ganji, D. Balarak, UV and visible light induced photodegradation of reactive red 198 dye and textile factory wastewater on Fe2O3/bentonite/TiO2 nanocomposite, Minerals 12 (2022) 1417.
[63] S.K. Maji, N. Mukherjee, A. Mondal, B. Adhikary, Synthesis, characterization and photocatalytic activity of α-Fe2O3 nanoparticles, Polyhedron 33 (2012) 145–149.
[64] S. Hojat Ansari, M. Giahi, Photochemical degradation of fluocinolone acetonidin drug in aqueous solutions using nanophotocatalyst ZnO doped by C, N, and S, Iran, J. Chem. Chem. Eng. 36 (2017) 183–189.
[65] A. Aboussabek, L. Boukarma, S. El Qdhy, A. Ousaa, M. Zerbet, M. Chiban, Experimental investigation, kinetics and statistical modeling of methylene blue removal onto Clay@ Fe3O4: batch, fixed bed column adsorption and photo-Fenton degradation studies, Case Stud. Chem. Environ. Eng. 9 (2024) 100580.
[66] Y. Wang, W. Li, A. Irini, A novel and quick method to avoid H2O2 interference on COD measurement in Fenton system by Na2SO3 reduction and O2 oxidation, Water Sci. Technol. 68 (2013) 1529–1535.
[67] B. Huang, Y. Liu, B. Li, H. Wang, G. Zeng, Adsorption mechanism of polyethyleneimine modified magnetic core–shell Fe 3 O 4@ SiO 2 nanoparticles for anionic dye removal, RSC Adv. 9 (2019) 32462–32471.
[68] D. Zhang, S. Lv, Z. Luo, A study on the photocatalytic degradation performance of a [KNbO 3] 0.9-[BaNi 0.5 Nb 0.5 O 3− δ] 0.1 perovskite, RSC Adv. 10 (2020) 1275–1280.
[69] X. Li, B. Xiao, M. Wu, L. Wang, R. Chen, Y. Wei, H. Liu, In-situ generation of multi-homogeneous/heterogeneous Fe-based Fenton catalysts toward rapid degradation of organic pollutants at near neutral pH, Chemosphere 245 (2020) 125663.
[70] Z. Heidari, R. Pelalak, R. Alizadeh, N. Oturan, S. Shirazian, M.A. Oturan, Application of mineral iron-based natural catalysts in electro-Fenton process: a comparative study, Catalysts 11 (2021) 57.
[71] G. Samiotis, A. Stimoniaris, I. Ristanis, L. Kemmou, C. Mavromatidou, E. Amanatidou, Application of metallic iron and ferrates in water and wastewater treatment for Cr (VI) and organic contaminants removal, Resources 12 (2023) 39.
[72] C. Xiao, S. Li, F. Yi, B. Zhang, D. Chen, Y. Zhang, H. Chen, Y. Huang, Enhancement of photo-Fenton catalytic activity with the assistance of oxalic acid on the kaolin–FeOOH system for the degradation of organic dyes, RSC Adv. 10 (2020) 18704–18714.
[73] H.G. Quynh, H. Van Thanh, N.T.T. Phuong, N.P.T. Duy, L.H. Hung, N. Van Dung, N.T.H. Duong, N.Q. Long, Rapid removal of methylene blue by a heterogeneous photo-Fenton process using economical and simple-synthesized magnetite–zeolite composite, Environ. Technol. Innov. 31 (2023) 103155.
[74] Q. Xiao, S. Yu, L. Li, T. Wang, X. Liao, Y. Ye, An overview of advanced reduction processes for bromate removal from drinking water: reducing agents, activation methods, applications and mechanisms, J. Hazard Mater. 324 (2017) 230–240.
[75] Y. Cao, J. Li, Y. Zhao, Y. Zhao, W. Qiu, S. Pang, J. Jiang, Degradation of metoprolol by UV/sulfite as an advanced oxidation or reduction process: the significant role of oxygen, J. Environ. Sci. 128 (2023) 107–116.
[76] S. Wu, L. Shen, Y. Lin, K. Yin, C. Yang, Sulfite-based advanced oxidation and reduction processes for water treatment, Chem. Eng. J. 414 (2021) 128872.
[77] S. Mahmoudi, S. Fadaei, E. Taheri, A. Fatehizadeh, T.M. Aminabhavi, Direct red 89 dye degradation by advanced oxidation process using sulfite and zero valent under ultraviolet irradiation: toxicity assessment and adaptive neuro-fuzzy inference systems modeling, Environ. Res. 211 (2022) 113059.
[78] V.N. Lima, C.S. Rodrigues, Y.B. Brandao, M. Benachour, L.M. Madeira, Optimisation of the degradation of 4-nitrophenol by Fenton's process, J. Water Process Eng. 47 (2022) 102685.
[79] A. Shokri, Application of Sono–photo-Fenton process for degradation of phenol derivatives in petrochemical wastewater using full factorial design of experiment, Int. J. Ind. Chem. 9 (2018) 295–303.
[80] I.K. Benramdane, N. Nasrallah, A. Amrane, M. Kebir, M. Trari, F. Fourcade, A.A. Assadi, R. Maachi, Optimization of the artificial neuronal network for the degradation and mineralization of amoxicillin photoinduced by the complex ferrioxalate with a gradual and progressive approach of the ligand, J. Photochem. Photobiol. Chem. 406 (2021) 112982.
[81] U.J. Ahile, R.A. Wuana, A.U. Itodo, R. Sha'Ato, R.F. Dantas, A review on the use of chelating agents as an alternative to promote photo-Fenton at neutral pH: current trends, knowledge gap and future studies, Sci. Total Environ. 710 (2020) 134872.
[82] Z. Hu, J. Shi, H. Yang, J. Huang, F. Sheng, How organic substances promote the chemical oxidative degradation of pollutants: a mini review, Sustainability 13 (2021) 10993.
[83] M. Kebir, I. kahina Benramdhan, N. Noureddine, H. Tahraoui, B. Nadia, B. Houssine, A. Rachid, J. Zhang, A.A. Assadi, L. Mouni, Sunlight Degradation and Mineralization of Food Dye Photoinduced by Homogenous Photo Fenton Fe (III) and Fe (II)/Complex: Surface Response Modeling, 2023.
[84] M. Kebir, I.-K. Benramdhan, N. Nasrallah, H. Tahraoui, N. Bait, H. Benaissa, R. Ameraoui, J. Zhang, A.A. Assadi, L. Mouni, Surface response modeling of homogeneous photo Fenton Fe (III) and Fe (II) complex for sunlight degradation and mineralization of food dye, Catal. Commun. 183 (2023) 106780.

[85] E. Clemente, E. Domingues, R.M. Quinta-Ferreira, A. Leitão, R.C. Martins, Solar photo-Fenton and persulphate-based processes for landfill leachate treatment: a critical review, Sci. Total Environ. (2023) 169471.
[86] B. Lin, S.G. Heijman, R. Shang, L.C. Rietveld, Integration of oxalic acid chelation and Fenton process for synergistic relaxation-oxidation of persistent gel-like fouling of ceramic nanofiltration membranes, J. Membr. Sci. 636 (2021) 119553.
[87] W. Remache, D.R. Ramos, L. Mammeri, H. Boucheloukh, Z. Marín, S. Belaidi, T. Sehili, J.A. Santaballa, M. Canle, An efficient green photo-Fenton system for the degradation of organic pollutants. Kinetics of propranolol removal from different water matrices, J. Water Process Eng. 46 (2022) 102514.
[88] U.J. Ahile, R.A. Wuana, A.U. Itodo, R. Sha'Ato, J.A. Malvestiti, R.F. Dantas, Are iron chelates suitable to perform photo-Fenton at neutral pH for secondary effluent treatment? J. Environ. Manag. 278 (2021) 111566.
[89] A. Hernández-Gordillo, P. Acevedo-Peña, M. Bizarro, S.E. Rodil, R. Gómez, Photoreduction of 4-Nitrophenol in the presence of carboxylic acid using CdS nanofibers, J. Mater. Sci. Mater. Electron. 29 (2018) 7345–7355.
[90] H. Dai, S. Xu, J. Chen, X. Miao, J. Zhu, Oxalate enhanced degradation of Orange II in heterogeneous UV-Fenton system catalyzed by Fe3O4@ γ-Fe2O3 composite, Chemosphere 199 (2018) 147–153.
[91] W. Huang, M. Luo, C. Wei, Y. Wang, K. Hanna, G. Mailhot, Enhanced heterogeneous photo-Fenton process modified by magnetite and EDDS: BPA degradation, Environ. Sci. Pollut. Res. 24 (2017) 10421–10429.
[92] B.M. Souza, M.W. Dezotti, R.A. Boaventura, V.J. Vilar, Intensification of a solar photo-Fenton reaction at near neutral pH with ferrioxalate complexes: a case study on diclofenac removal from aqueous solutions, Chem. Eng. J. 256 (2014) 448–457.
[93] A.J. Exposito, J.M. Monteagudo, A. Durán, I. San Martín, L. González, Study of the intensification of solar photo-Fenton degradation of carbamazepine with ferrioxalate complexes and ultrasound, J. Hazard Mater. 342 (2018) 597–605.
[94] A. Das, M.K. Adak, Photo-catalyst for wastewater treatment: a review of modified Fenton, and their reaction kinetics, Appl. Surf. Sci. Adv. 11 (2022) 100282.
[95] H. Wang, N. Zhang, G. Cheng, H. Guo, Z. Shen, L. Yang, Y. Zhao, A. Alsaedi, T. Hayat, X. Wang, Preparing a photocatalytic Fe doped TiO2/rGO for enhanced bisphenol A and its analogues degradation in water sample, Appl. Surf. Sci. 505 (2020) 144640.
[96] H. Yi, D. Ma, X. Huo, L. Li, M. Zhang, X. Zhou, F. Xu, H. Yan, G. Zeng, C. Lai, Facile introduction of coordinative Fe into oxygen-enriched graphite carbon nitride for efficient photo-Fenton degradation of tetracycline, J. Colloid Interface Sci. 660 (2024) 692–702.
[97] S. Wang, D. Hu, Y. Liu, H. Xiong, Synthesis of ferrihydrite/polyaniline composite using waste Fe (III)/EPS-cultures with polyaniline and its application for tetracycline photo-Fenton degradation, J. Environ. Chem. Eng. (2024) 112180.
[98] R. Wang, Y. Chu, H. Zhang, Comprehensive evaluation of the catalytic activity of alpha-ferric oxide in photocatalysis, Fenton-like and photo-Fenton systems for organics degradation: performance and in-depth mechanism consideration, J. Environ. Chem. Eng. (2024) 112479.
[99] T. Mohapatra, P. Ghosh, Photo-Fenton remediation of textile wastewater in fluidized-bed reactor using modified laterite: hydrodynamic study and effect of operating parameters, Chem. Eng. J. (2023) 145324.
[100] D. Vione, Insights into the time evolution of slowly photodegrading contaminants, Molecules 26 (2021) 5223.